Rhodolith-forming coralline red algae in the CaCO₃ biofactory — A case study from the Serravallian of tropical northeastern Indian Ocean

Rikee DEY, Daniela BASSO, Arindam CHAKRABORTY,
Lopamudra ROY, Ajoy Kumar BHAUMIK & Amit K. GHOSH

PUBLICATIONS SCIENTIFIQUES

MUSÉUM NATIONAL D'HISTOIRE NATURELLE

Rhodolith-forming coralline red algae in the CaCO₃ biofactory — A case study from the Serravallian of tropical northeastern Indian Ocean

Rikee DEY
Birbal Sahni Institute of Palaeosciences, 53 University Road,
Lucknow — 226 007, Uttar Pradesh (India)
and Department of Applied Geology, Indian Institute of Technology
(Indian School of Mines), Dhanbad — 826 004, Jharkhand (India)

Daniela BASSO
University of Milano-Bicocca, Department of Earth and Environmental Sciences,
Piazza della Scienza 4, I-20126, Milano (Italy)

Arindam CHAKRABORTY
Birbal Sahni Institute of Palaeosciences, 53 University Road,
Lucknow — 226 007, Uttar Pradesh (India)
and Department of Geology, Faculty of Science, Universiti Malaya,
50603 Kuala Lumpur (Malaysia)

Lopamudra ROY
Birbal Sahni Institute of Palaeosciences, 53 University Road,
Lucknow — 226 007, Uttar Pradesh (India)
and Centre of Advanced Study in Geology, University of Lucknow,
Lucknow — 226007, Uttar Pradesh (India)

Ajoy Kumar BHAUMIK
Department of Applied Geology, Indian Institute of Technology (Indian School of Mines),
Dhanbad — 826 004, Jharkhand (India)

Amit K. GHOSH
Birbal Sahni Institute of Palaeosciences, 53 University Road,
Lucknow — 226 007, Uttar Pradesh (India)
akghosh_in@yahoo.com, amitk_ghosh@bsip.res.in (corresponding author)

ABSTRACT
Rhodolith-forming non-geniculate coralline red algae have been recorded from the Long Formation, exposed in four different outcrops at Little Andaman Island (Hut Bay) in the northeastern Indian Ocean. The non-geniculate corallines are represented by species of *Sporolithon* Heydrich, 1897, *Mesophyllum* Lemoine, 1928, *Lithothamnion* Heydrich, 1897, *Phymatolithon* Foslie, 1898,

Lithoporella (Foslie) Foslie, 1909, *Spongites* Kützing, 1841, *Neogoniolithon* Setchell & Mason, 1943 and *Lithophyllum* Philippi, 1837. The algal assemblages also include geniculate corallines belonging to the genera *Amphiroa* Lamouroux, 1812 and *Corallina* Linnaeus, 1758. In addition, larger benthic foraminifers and few planktonic foraminifers also have been identified in thin section analysis. Based on the earlier study carried out on planktonic foraminifers, the Long Formation has been dated as Serravallian (late middle Miocene) and chronostratigraphically, the Long Formation has been included in the Ongeian Regional Stage. In the rhodolith-forming non-geniculate corallines, various growth forms and taphonomic features have been recognized. Diagenesis affected the studied material by micritization, cementation and compaction. The four outcrops are dominated by bioclastic wackestone and packstone composed of coralline red algae, benthic and planktonic foraminifers, echinoid spines and unidentified coral fragments. The rhodolith-forming coralline red algae, the growth forms and taphonomic features in non-geniculate corallines and the characteristic benthic foraminifers are indicative of a moderate energy depositional environment. This study indicates that the carbonate production was considerably high during the Serravallian of the tropical northeastern Indian Ocean.

RÉSUMÉ
Algues rouges corallines formant des rhodolithes dans la biousine de CaCO₃ – Une étude de cas du Serravallien du nord-est de l'océan Indien tropical.
Des algues rouges coralliennes non géniculées formant des rhodolithes ont été enregistrées dans la formation de Long, exposées dans quatre affleurements différents sur l'île Little Andaman (Hut Bay). Les corallines non géniculées sont représentées par des espèces de *Sporolithon* Heydrich, 1897, *Mesophyllum* Lemoine, 1928, *Lithothamnion* Heydrich, 1897, *Phymatolithon* Foslie, 1898, *Lithoporella* (Foslie) Foslie, 1909, *Spongites* Kützing, 1841, *Neogoniolithon* Setchell & Mason, 1943 et *Lithophyllum* Philippi, 1837. Les assemblages d'algues comprennent également des corallines géniculées appartenant aux genres *Amphiroa* Lamouroux, 1812 et *Corallina* Linnaeus, 1758. De plus, des foraminifères benthiques plus grands et quelques foraminifères planctoniques ont également été identifiés dans l'analyse des lames minces. Sur la base de l'étude antérieure réalisée sur les foraminifères planctoniques, la Formation de Long a été datée du Serravallien (Miocène moyen tardif) et chronostratigraphiquement, la Formation de Long a été incluse dans le Stade Régional Ongeien. Dans les corallines non géniculées formant des rhodolithes, diverses formes de croissance et caractéristiques taphonomiques ont été reconnues. La diagenèse affecte le matériau étudié par micritisation, cimentation et compaction. Les quatre affleurements sont dominés par du wackestone et du packstone bioclastiques composés d'algues rouges coralliennes, de foraminifères benthiques et planctoniques, d'épines d'échinoïdes et de fragments de corail non identifiés. Les algues rouges coralliennes formant des rhodolithes, les formes de croissance et les caractéristiques taphonomiques des corallines non géniculées et les foraminifères benthiques caractéristiques indiquent un environnement de dépôt d'énergie modérée. Cette étude montre que la production de carbonate était considérablement élevée au cours du Serravallien du nord-est tropical de l'océan Indien.

INTRODUCTION

Rhodoliths are unattached nodules composed of calcareous red algae, more commonly Corallinophycidae Le Gall & Saunders, 2007 (coralline algae) and species of family Peyssonneliaceae Denizot, 1968. The name rhodolite was coined by Bosellini & Ginsburg (1971) and they defined them as a spherical form of calcareous nodules and detached branched growths which are principally composed of coralline red algae. Binda (1973) commented that the usage of the term rhodolite is ambiguous, as it is traditionally used for a variety of garnet. Subsequently, Ginsburg & Bosellini (1973) proposed the name rhodolith for those nodules. Earlier, Barnes *et al.* (1970) also used the term rhodolith to indicate red algal nodules, without any definition. Rhodoliths are widely distributed and their excellent fossil record can provide valuable insights into palaeoecology and palaeobiogeography (Bosellini & Ginsburg 1971; Adey & Macintyre 1973; Bosence 1983a, b; Basso & Tomaselli 1994; Aguirre *et al.* 2000, 2012; Basso *et al.* 2009, 2017; Rebelo *et al.* 2014). Rhodoliths are sensitive to burial and smothering, and need active hydrodynamics or bioturbation to prevent their detrimental effects (Bosence 1983a, b; Braga & Martín 1988; Littler *et al.* 1990; Foster *et al.* 1997; Marrack 1999; Foster 2001; Braga *et al.* 2003; Bracchi *et al.* 2019, 2022). Geographically, rhodolith beds are distributed from the tropical to polar oceans and from the intertidal zones down to about 200 m of water depth (Foster 2001; Nelson 2009).
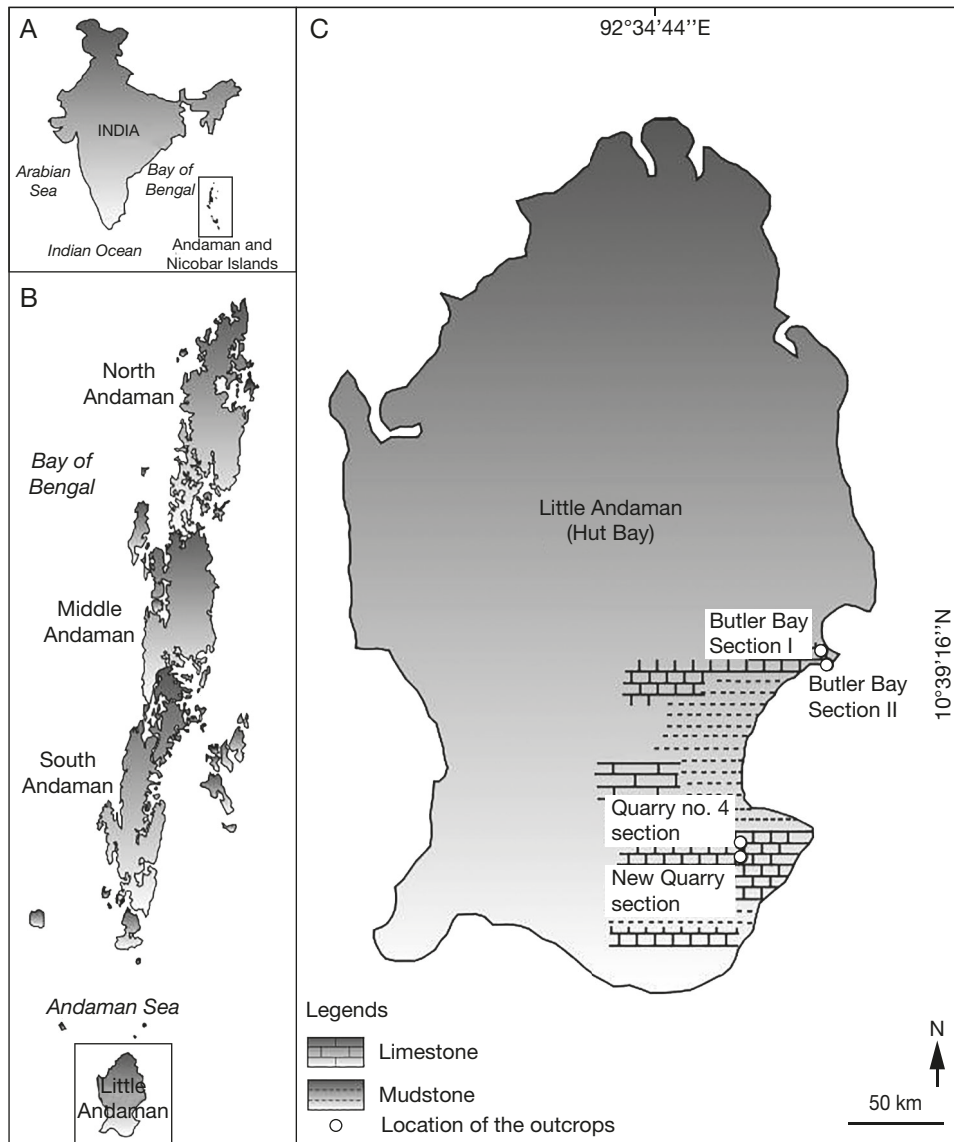
FIG. 1. — **A**, Andaman and Nicobar Islands in the northeastern Indian Ocean (map not to scale); **B**, islands of Ritchies Archipelago (map not to scale); **C**, geological map of Little Andaman Island showing the sampling sites (modified after Sharma & Srinivasan 2007).

According to Bosellini & Ginsburg (1971), rhodolith shape is dependent on the water movement. In general, spheroidal and ellipsoidal rhodoliths are formed in moderate to high-energy environment. On the other hand, flat discoidal and ameboidal rhodoliths are more stable and ellipsoidal rhodoliths are more easily transported than spheroidal ones (Bosence 1976). Accordingly, discoidal rhodoliths are expected to be abundant in calm water; whereas, ellipsoidal and spheroidal rhodoliths should be dominant in moderate to high energy conditions. However, a growing body of evidence demonstrates that the relationship between rhodolith shape and hydrodynamics is not straightforward (Adey & Macintyre 1973; Steller & Foster 1995; Bracchi *et al.* 2022). The occurrence of a lithic nucleus may control the final shape and change the mean density of the rhodoliths, influencing the frequency of displacement by currents, depending on the stream competence (Basso & Tomaselli 1994; Basso *et al.*

2009). Although the growth form of the composing coralline species is also one of the obvious controls of rhodolith morphology (Nebelsick & Bassi 2000), field data showed a correspondence of spherical and compact rhodoliths with higher current velocity, while open structures of unattached branches are related to weaker, occasional currents (Basso 1998; Bracchi *et al.* 2022).

Coralline algae are one of the most significant carbonate producers of the photic zone in modern oceans (Basso 2012; Riosmena-Rodríguez 2017). In the tropical shelf environments, coralline algae are considered one of the most important carbonate producers and habitat formers that contribute to reefs and rhodolith beds. The global carbonate (CO$_3^{2-}$) budget is predominantly influenced by calcium carbonate (CaCO$_3$) production by marine biota. Distribution of coralline red algae ranges from tropical to polar zones and they can survive in low light intensity (Adey & Macintyre 1973; Coletti

et al. 2015) owing to the presence of phycoerythrin, a unique photosynthetic pigment (Lee 1989; Van Den Hoek *et al.* 1995). During the Late Cretaceous their occurrence has been recorded in the shelf environment and in the Oligocene they were widespread in the photic zone (Nebelsick *et al.* 2005). In the Cenozoic, corallines became abundant throughout the globe (Bourrouilh & Hottinger 1988; Halfar & Mutti 2005; Braga *et al.* 2010; Pomar *et al.* 2017).

In the Mediterranean, Indo-Pacific and Caribbean regions rhodalgal carbonate factories were well developed during the Miocene (Civitelli & Brandano 2005; Braga *et al.* 2010). In the northeast Indian Ocean, middle Miocene algal-foraminiferal limestones are exposed in different islands of Andaman and Nicobar Group (Sharma & Srinivasan 2007). Specifically, in the Little Andaman Island (Hut Bay) of the Andaman Group there are previous records of coralline red algae from the Serravallian limestones (Sarkar & Ghosh 2015; Sarkar *et al.* 2016; Ghosh *et al.* 2017 and references therein), however, rhodolith-forming coralline red algae were not assessed.

The present study is focused on the Serravallian of Long Formation outcropping at four sections in Little Andaman Island. The aim is to analyze the coralline red algal association forming the rhodoliths, to identify the different facies recorded in the four outcrops, to decipher the depositional environment in which the rhodoliths were formed, and to reconstruct the main steps of their diagenetic history.

GEOGRAPHY AND GEOLOGICAL SETTING

The Andaman-Nicobar region is one of the most seismically active subduction zones in this part on Earth, situated between 6° and 14° N in the northeastern Indian Ocean (Fig. 1A). Gaubolambe, the native name of Little Andaman Island (Hut Bay) is derived from the Onge tribes and this is the fourth largest island among the Andaman Group that occupies an area of about 707 km². The island is located about 120 km south of capital city Port Blair (Fig. 1B). The Little Andaman Island (Hut Bay), the southernmost island of the Andaman Group is located between the South Andaman and Car Nicobar Island. Geographically, Little Andaman Island is situated between 10°30'N-10°54'N, and 92°20'E-92°37'E, which is separated from the South Andaman by the Duncan Passage and Car Nicobar by the Ten-Degree Channel respectively (Fig. 1C). The Long Formation is well exposed in this island which has been designated as Ongeian Regional Chronostratigraphic Stage (Sharma & Srinivasan 2007). The Long Formation was dated as Serravallian (13.9 to 11.5 Ma) based on the planktonic foraminiferal zones *Fohsella* (synonym of *Globorotalia*) *fohsi fohsi* and *Fohsella* (synonym of *Globorotalia*) *fohsi robusta* respectively (Srinivasan 1988; Sharma & Srinivasan 2007). The sediments belonging to the Long Formation are exposed in the two cliffs of Butler Bay and two limestone quarries, i.e., Limestone Quarry No. 4 and New Quarry on the Little Andaman Island (Fig. 1C). This study has been carried out from four different outcrops: Butler Bay Section-I and Section-II, Hut Bay Quarry No. 4 Section and New Quarry Section. The two outcrops of Butler Bay (Butler Bay Section-I 10°39.482'N, 92°34.937'E and Butler Bay Section-II 10°39.516'N, 92°34.907'E) are lithologically comprised of dark grey to white mottling hard fossiliferous limestone, with significantly high (45%) vuggy as well as moldic porosity (Srinivasan & Chatterjee 1981; Sarkar & Ghosh 2015) rich in coralline red algae forming rhodoliths, halimedacean green algae (Ghosh *et al.* 2017) and foraminifers (Fig. 2A, B). Samples collected from Hut Bay Quarry No. 4 (10°34.568'N, 92°32.491'E) are lithologically distinguished on the base of their dark grey fossiliferous limestone with rhodoliths, passing up section to a white colored foraminiferal limestone, which in turn is overlain by concretions with coral rags and bioherms (Fig. 2C). The lower part of New Quarry Section (10°34.500'N, 92°32.480'E) comprises of yellowish-white algal-foraminiferal limestone with rhodoliths, whereas the upper part is overlain by concretions with coral rubble and bioherms (Fig. 2D).

MATERIAL AND METHODS

Samples were collected from two outcrops on Butler Bay (Sections I and II) (Fig. 2A, B) and two outcrops situated at Hut Bay Limestone Quarry (HB Quarry No. 4 and New Quarry Section) (Fig. 2C, D). The Butler Bay Section-I is *c.* 15 m thick and twenty-seven samples were collected from this outcrop (Sample no. 8114/01 to 8114/27). Thirty samples were collected from the Butler Bay Section-II which is *c.* 7 m in thickness (Sample no. 8898/01 to 8898/30). Eight samples were collected from HB Quarry No. 4 which is *c.* 11 m in thickness (Sample no. 8900/01 to 8900/08). The thickness of New Quarry Section is *c.* 3.5 m, from where seven samples were collected (Sample no. 8901/01 to 8901/08).

For the description of coralline microanatomy, the term hypothallus corresponds to the ventral core of cell filaments (VC), and the term perithallus corresponds to the peripheral filaments (PF) arising from the ventral core (Hrabovský *et al.* 2015). Other anatomical characters are described based on Hrabovský *et al.* (2015). Higher rank taxonomy follows AlgaeBase (Guiry & Guiry 2018).

Palaeontological thin sections (*c.* 2.5 × 3.5 cm) were prepared from each sample containing rhodoliths. Petrographic thin sections measuring 30 μm in thickness were prepared for microscopic study. Four microscopic slides from each sample were studied by Olympus BX 50 light microscope. The cells and conceptacle dimensions were measured under light microscope at magnifications of 4×, 10×, 20× and 40×. The study of thin sections with uniform microscopic field area is necessary to understand the diversity of the biotic components. All the photomicrographs were taken using Olympus DP 26 Digital camera having CellSens Standard software attached to the Olympus BX 50 light microscope. The figured slides are preserved in the repository of Birbal Sahni Institute of Palaeosciences, Lucknow.
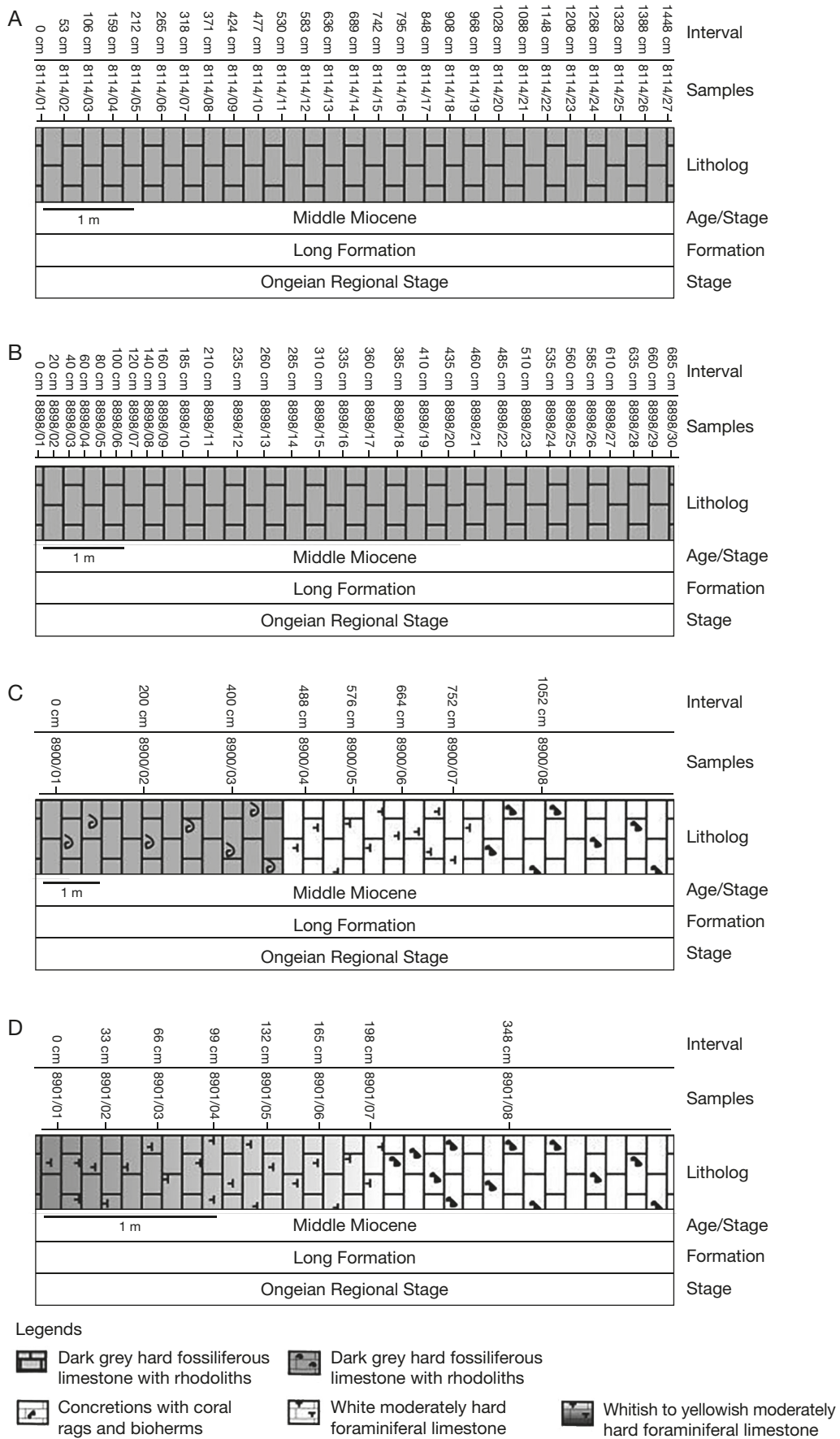
FIG. 2. — Lithologs of the outcrops: **A**, Butler Bay Section-I; **B**, Butler Bay Section-II; **C**, Hut Bay Quarry No. 4 Section; **D**, New Quarry Section.

RESULTS

SYSTEMATIC PALAEONTOLOGY

Order CORALLINALES Silva &
Johansen, 1986
Family HAPALIDIACEAE Gray, 1864
Genus *Lithothamnion* Heydrich, 1897

?*Lithothamnion valens*
(Fig. 3A, B)

DESCRIPTION
Thallus fruticose, with protuberances 2898-3017 µm in length and 826-1391 µm in diameter. Thallus monomerous, non-coaxial, cell fusions present both in the VC and PF. Cells of the VC measure 16 to 18 µm in length and 8 to 11 µm in diameter (Table 1). Cells of the PF 8 to 15 µm in length and 8 to 10 µm in diameter (Table 1), squarish to rectangular in shape. Conceptacles not observed.

REMARKS
The vegetative anatomy of the described specimens resembles to some extent to that of *Lithothamnion valens* Foslie (1909) in having large branched thallus, presence of zonation in the PF and numerous and multiple cell fusions (Basso *et al.* 1997). However, owing to absence of conceptacles, this form is only tentatively assignable to the genus *Lithothamnion*. *Lithothamnion valens* is one of the most common species of non-geniculate corallines identified in the Austrian Leitha Limestone (Basso *et al.* 2008). This species commonly shows a free-living, branching growth-form and is endemic in present day Mediterranean Sea. Moussavian (1984) reported its oldest occurrence from the Priabonian of Northern Calcareous Alps. During lower to middle Miocene *L. valens* was distributed from Iraq to the Tertiary Piedmont Basin. However, the species was restricted to the Mediterranean region starting from the upper Miocene (Basso *et al.* 1997).

Genus *Phymatolithon*
Foslie, 1898

Phymatolithon sp.
(Fig. 3C, D)

DESCRIPTION
Growth form encrusting to foliose, thallus monomerous; the VC is non-coaxial with zonations in PF. The cells of VC more or less rectangular, measuring 16-20 µm in length and 12-14 µm in diameter (Table 1). Peripheral filaments composed of 6 to 12 cells thick, each zone showing a gradual transition of long and short cells, cells of the peripheral filaments measure 8-10 µm in length and 6-9 µm in diameter. Cell fusions present in both VC and PF. Epithallial cells are visible and non-flared in some specimens. Tetra/bisporangial conceptacles are multiporate, buried within the thallus, conceptacle roof distinct, conceptacles raised above the thallus surface. Conceptacle chambers 360 to 480 µm in diameter and 140 to 180 µm in height (Table 1).

REMARKS
The illustrated specimens are similar to the *Phymatolithon calcareum* (Pallas) Adey & McKibbin described from the upper Miocene of Santa Maria Island, Azores, NE Atlantic Ocean (Rebelo *et al.* 2014), but the encrusting to foliose growth form does not match the description of *P. calcareum,* which is commonly fruticose. For this reason, we leave this specimen in open nomenclature. According to Rasser & Piller (1999) the genus *Phymatolithon* is common in the late Eocene of the Austrian Molasse Zone.

Family MESOPHYLLUMACEAE Schneider &
Wynne, 2019
Genus *Mesophyllum* Lemoine, 1928

Mesophyllum sp.
(Fig. 3E)

DESCRIPTION
Growth form encrusting to warty, thallus measures 1141-1322 µm in length and 600-715 µm in thickness, monomerous. Cells of the VC are coaxial, more or less rectangular in shape and measures 12 to 24 µm in length and 6 to 10 µm in diameter (Table 1). Cells of the PF are 8 to 25 µm in length and 6 to 20 µm in diameter (Table 1). A wavy zonation is present in the PF. Cell fusions clearly discernible both in the VC and PF. Epithallial cells not clearly visible.

REMARKS
Based on the presence of cell fusions both in VC and PF, zonations in the PF and monomerous thallus with coaxial VC the specimen is confidently assigned to the genus *Mesophyllum.* The vegetative anatomical features and growth form recall *Mesophyllum curtum* Lemoine, re-described from the Tortonian of Algeria (Aguirre & Braga 1998) and from the Langhian of southern Moravia, Carpathian Foredeep, Czech Republic (Hrabovský *et al.* 2015).

Mesophyllum roveretoi
Conti, 1943
(Fig. 3F)

Mesophyllum roveretoi Conti, 1943: 55.
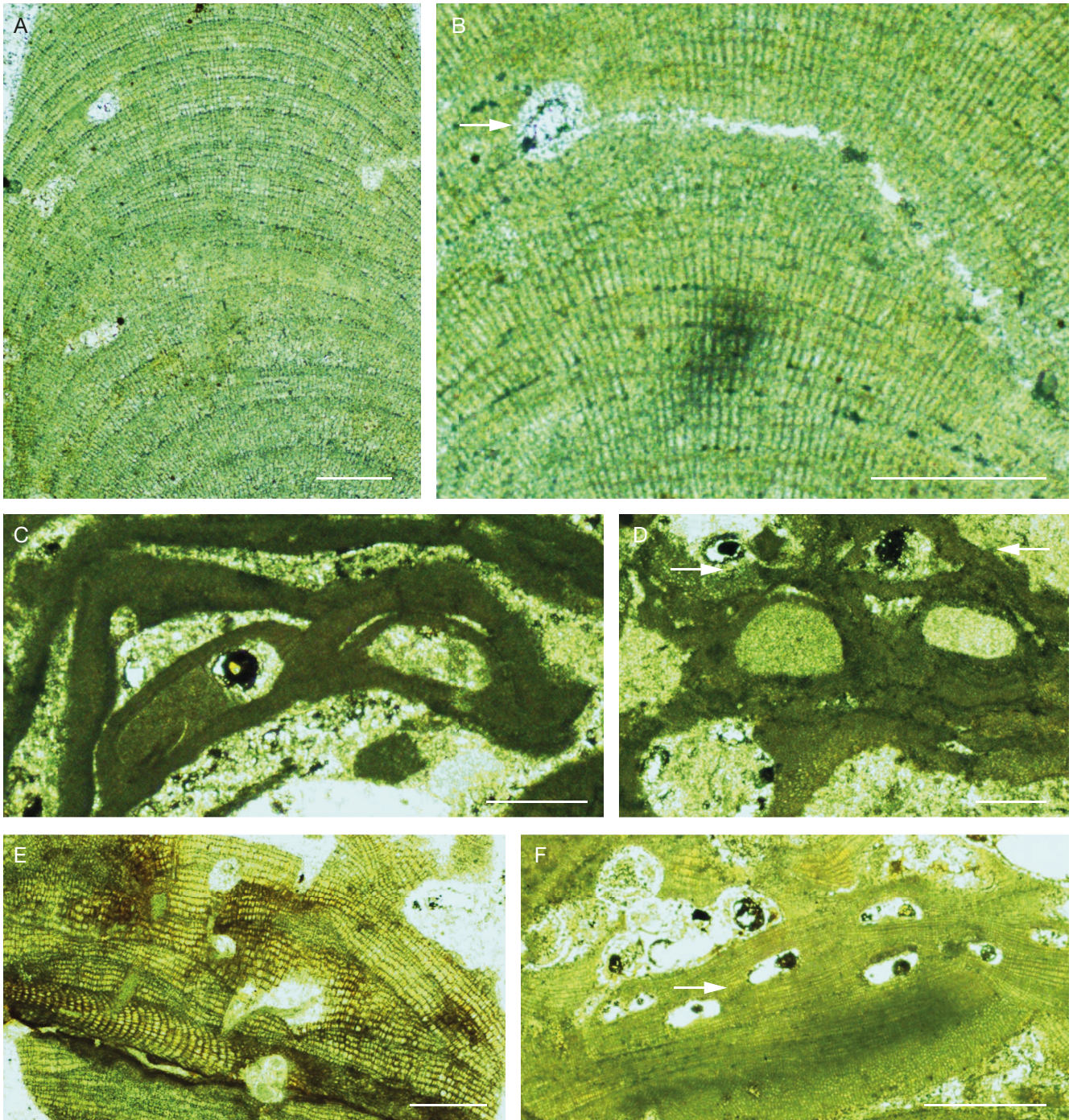
Fig. 3. — **A**, **B**, ?*Lithothamnion valens* (BSIP Slide No. 17030) encrusting and layered growth form, monomerous non-coaxial thallus with cell fusions in VC and PF; **C**, **D**, *Phymatolithon* sp. (BSIP Slide No. 17038, 17038) growth form encrusting to foliose, tetra/bisporangial multiporate conceptacles buried within the thallus; **E**, *Mesophyllum* sp. (BSIP Slide No. 17040) encrusting to warty growth form, coaxial VC and wavy zonation in PF; **F**, *Mesophyllum roveretoi* Conti, 1943 (BSIP Slide No. 17028) coaxial ventral core with multiporate conceptacles. **Arrows**: B, D, indicate chemical dissolution; **F**, indicates cell fusion. Scale bars: A, B, E, 200 μm; C, D, 250 μm; F, 500 μm.

DESCRIPTION

Protuberances with a lumpy growth form. Thallus monomerous with presence of cell fusions in both VC and PF. The VC is coaxial (Fig. 3F) and the cells of VC measure 14-20 μm in length and 8-12 μm in diameter. The cells of PF measuring 14-31 μm in length and 8-28 μm in diameter. Multiporate conceptacles are flat, 229-235 μm in diameter and 71-96 μm in height (Table 1).

REMARKS

The features of thallus organization, growth form, anatomical features and nature of conceptacles are consistent with the description of *Mesophyllum roveretoi* provided by Basso *et al.* (2008) from the Miocene "Lithothamnium Limestone" of northern Croatia. The taxon stratigraphically ranges from the upper Eocene to the middle Miocene (Conti 1946; Fravega *et al.* 1987) (Table 2).

Family MASTOPHORACEAE Townsend & Huisman, 2018
Subfamily MASTOPHOROIDEAE Setchell, 1943
Genus *Lithoporella* Foslie, 1909

Lithoporella melobesioides (Foslie) Foslie, 1909
(Fig. 4A, B)

Mastophora melobesioides Foslie, 1903: 24.

Lithoporella melobesioides (Foslie) Foslie, 1909: 59.

DESCRIPTION
Encrusting growth form, forming either single thallus or multiple overgrowth, primigenous filaments composed of large vertically elongated cells forming unistratose layers, thallus dimerous, cells of the VC measuring 12 to 18 µm in length and 22 to 38 µm in diameter, postigenous filaments arise from the primigenous filaments and mostly occur around the conceptacles. Cells of the postigenous filaments measure 16 to 32 µm in length and 8 to 20 µm in diameter. Conceptacles are uniporate, measuring 174 to 400 µm in diameter and 71 to 140 µm in height (Table 1).

REMARKS
According to Woelkerling (1988) the status of most of the species of *Lithoporella* is uncertain, though *Lithoporella melobesioides* has been described as fossils from the Palaeogene and Neogene sediments from different parts of the world. Our observations confirm the description provided by Rasser & Piller (1999) for the late Eocene material of the Austrian Molasse zone. The earliest record of the taxon is from the late Jurassic (Aguirre *et al.* 2000). In India, *Lithoporella melobesioides* has been recorded earlier from the late Eocene (Sarma *et al.* 2014), Miocene to Holocene (Kundal *et al.* 2011, 2016) (Table 2).

Suborder CORALLININAE Athanasiadis, 2016
Family SPONGITIDACEAE Kützing, 1843
Subfamily NEOGONIOLITHOIDEAE Kato & Baba, 2011
Genus *Neogoniolithon* Setchell & Mason, 1943

Neogoniolithon sp.
(Fig. 4C)

DESCRIPTION
Thallus encrusting, monomerous, dorsiventral with coaxial ventral core. The cells of VC are 10 to 28 µm in length and 7 to 12 µm in diameter and PF cells are 9 to 20 µm in length and 5 to 11 µm in diameter. Cell fusions present both in VC and PF. Conceptacles uniporate, 550 to 600 µm in diameter and 200 to 300 µm in height. Epithallial cells not identified (Table 1).

REMARKS
The species has the characteristic features of the genus *Neogoniolithon*, but this form is not comparable to any earlier known species of the genus, though, it has some resemblance with *Neogoniolithon contii* Mastrorilli, 1967 reported by Quaranta

et al. (2007) from the Oligocene of NW Italy and northern Slovenia (Gale 2009) including the transition from coaxial to non-coxial and cell fusions both in VC and PF (Fig. 4C).

Genus *Spongites* Kützing, 1841

Spongites fruticulosus Kützing, 1841
(Fig. 4D, E)

Spongites fruticulosus Kützing, 1841: 33.

Lithophyllum albanense Lemoine, 1924: 281.

Spongites albanensis (Lemoine) Braga, Bosence & Steneck, 1993: 544, pl. 2, figs 1, 3, 4.

DESCRIPTION
Thallus encrusting, monomerous; non-coaxial VC, cells of the VC measure 16 to 24 µm in length and 12 to 18 µm in diameter. Cells of PF irregularly arranged with variable shapes that measure 12 to 22 µm in length and 8 to 18 µm in diameter. Epithallial cells flattened to round, measuring 5 to 7 µm long and 8 to 14 µm in diameter. Cell fusions are present both in the PF and VC (Table 1). Uniporate conceptacles raised above the thallus surface, cell linings in the pore canals more or less parallel to the roof of the conceptacle.

REMARKS
The specimens resemble the material described from the middle Miocene of Gârbova de Sus Formation, Transylvanian Basin, Romania (Chelaru & Bucur 2016). *Spongites fruticulosus* Kützing stratigraphically ranges from the Oligocene to Recent (Chelaru & Bucur 2016 and references therein). This species is widespread in the Mediterranean Sea as a rhodolith-forming coralline alga (Basso & Rodondi 2006) (Table 2).

Family LITHOPHYLLACEAE Athanasiadis, 2016
Subfamily LITHOPHYLLOIDEAE Setchell, 1943
Genus *Titanoderma* Nägeli, 1858

Titanoderma pustulatum (Lamouroux) Nägeli, 1858
(Fig. 4F)

Melobesia pustulata Lamouroux, 1816: 315.

Titanoderma pustulatum (Lamouroux) Nägeli, 1858: 532.

DESCRIPTION
Encrusting growth form, thallus dimerous, dorsiventral. Cells of VC 12 to 18 µm in length and 8 to 15 µm in diameter, palisade-like. Cells of PF are more or less squarish to rectangular, measuring 7 to 18 µm in length and 8 to 16 µm in diameter. Cell fusions occurring both in VC and PF. Epithallial cells are poorly preserved. Conceptacles uniporate, rose above the thallus surface, with chambers appearing hemispherical to elongated in section. Conceptacle chambers measure 110 to 140 µm in diameter and 72 to 94 µm in height (Table 1).
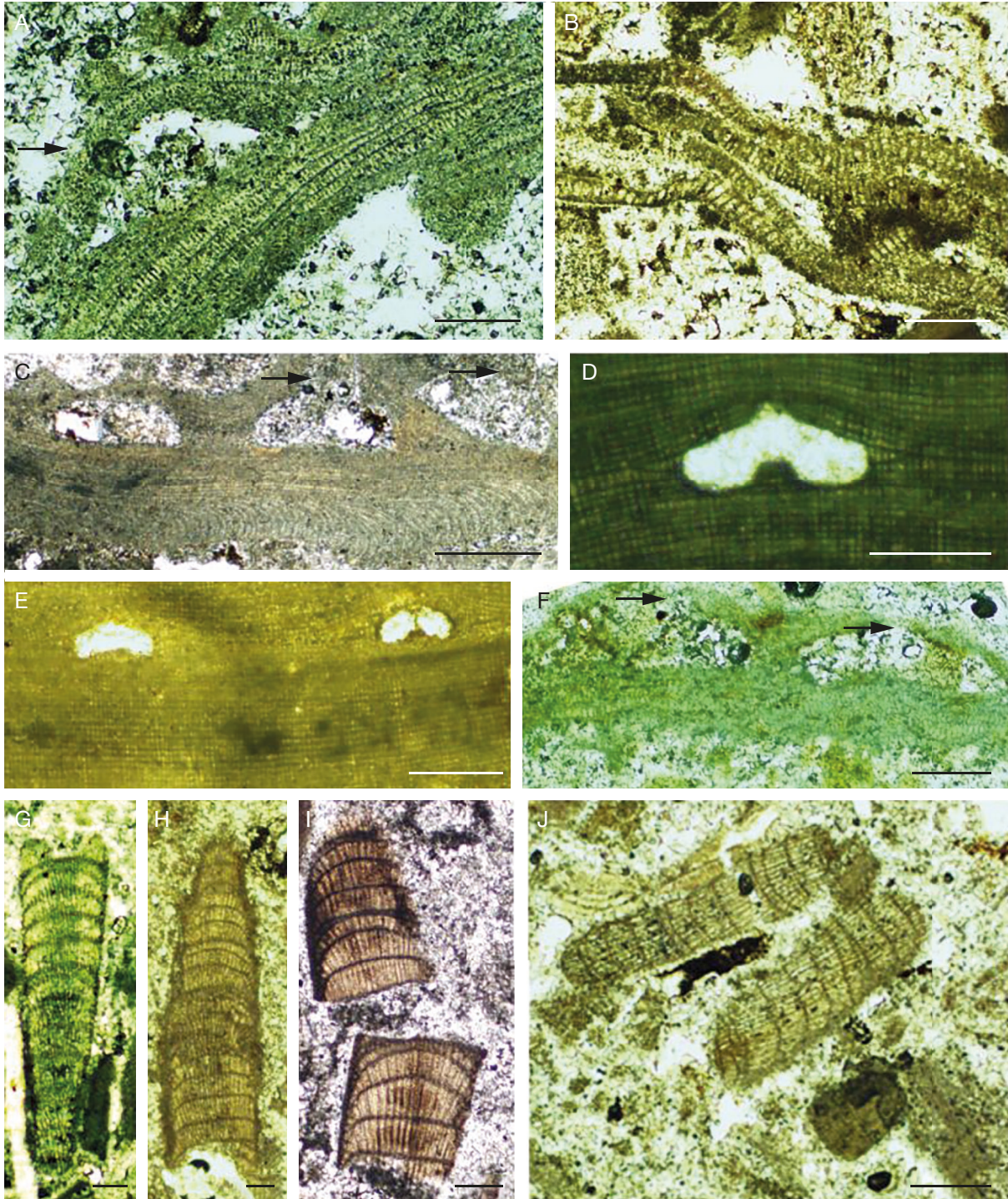
FIG. 4. — **A**, **B**, *Lithoporella melobesioides* (Foslie) Foslie, 1909 (BSIP Slide No. 17025, 17026) encrusting growth form, dimerous thallus and uniporate conceptacles; **C**, *Neogoniolithon* sp. (BSIP Slide No. 17029) thallus encrusting, cell fusions in ventral core (VC) and peripheral filaments (PF), conceptacles multiporate; **D**, **E**, *Spongites fruticulosus* Kützing, 1841 (BSIP Slide No. 17038, 17042) thallus encrusting, monomerous, conceptacles uniporate; **F**, *Titanoderma pustulatum* (Lamouroux) Nägeli, 1858 (BSIP Slide No. 17031, 17032) encrusting growth form, thallus dimerous, cell fusions in VC and PF, conceptacles uniporate; **G**-**J**, *Amphiroa* sp. (BSIP Slide No. 17036, 17024); **I**, *Amphiroa* sp. showing fragmentation; **J**, *Amphiroa* sp. showing disarticulation. **Arrows**: A, C, F, indicate chemical dissolution. Scale bars: A, B, D, J, 200 µm; C, E, 500 µm; F-I, 100 µm.

REMARKS

This non-endophytic species of *Titanoderma* shows the growth-form, size and shape of the conceptacle chamber and pore canal, conceptacle roof and thickness of the thallus that resemble

Titanoderma pustulatum, as described by previous authors (Chamberlain & Irvine 1994; Harvey *et al.* 2009; Van Der Merwe & Maneveldt 2015). The oldest record of *T. pustulatum* is from the early Oligocene of Iran (Basso *et al.* 2019) (Table 2).

TABLE 1. — Comparison of biometric measurements of the identified geniculate and non-geniculate coralline algae. Abbreviations: **D**, diameter; **H**, height; **L**, length; **PF**, peripheral filaments; **Po**, postigenous filaments; **Pr**, primigenous filaments; **VC**, ventral core.

Taxa	Features/ Characteristics	Dimensions	Number of measuments (n)	Range	Mean (M)	Standard Deviation (SD)
?*Lithothamnion valens* (Fig. 3A, B)	VC	L	15	16 to 18 µm	16.8	0.74
		D	15	8 to 11 µm	9.2	1.1
	PF	L	30	8 to 15 µm	10.6	2.41
		D	30	8 to 10 µm	8.8	0.74
	Multiporate conceptacles	D	5	84 to 117 µm	96.6	12.611
		H	5	50 to 91 µm	70.2	14.42
	Protuberances	L	3	2898 to 3017 µm	2942.6	54.08
		D	3	826 to 1391 µm	1072	236
Phymatolithon sp. (Fig. 3C, D)	VC	L	20	16 to 20 µm	18	1.67
		D	20	12 to 14 µm	12.8	0.74
	PF	L	50	8 to 10 µm	8.8	0.74
		D	50	6 to 9 µm	7.4	1.01
	Epithallial cells	L	9	8 to 15 µm	10.6	2.41
		D	9	± 5 µm	−	−
	Multiporate conceptacles	D	10	360 to 480 µm	400	42.4
		H	10	140 to 180 µm	160	14.1
Mesophyllum sp. (Fig. 3E)	VC	L	25	12 to 24 µm	18	9.4
		D	25	6 to 10 µm	8	1.41
	PF	L	50	8 to 25 µm	15.6	6.2
		D	50	6 to 20µm	12.8	4.7
	Multiporate conceptacles	D	3	140 to 180 µm	160	14.14
		H	3	85 to 140 µm	115	22.72
	Thallus	L	3	1141 to 1322 µm	1221	75.36
		D	3	600 to 715 µm	643.3	51.456
Mesophyllum roveretoi Conti, 1943 (Fig. 3F)	VC	L	20	14 to 20 µm	16.6	2.15
		D	20	8 to 12 µm	10	1.41
	PF	L	20	14 to 31 µm	21	6.35
		D	20	8 to 28 µm	17.2	7.98
	Multiporate conceptacles	D	3	229 to 235	231	2.6
		H	3	71 to 96	82.3	10.3
Lithoporella melobesiodies (Foslie) Foslie, 1909 (Fig. 4A, B)	Pr	L	15	12 to 18 µm	15.6	3.2
		D	15	22 to 38 µm	31.6	8.5
	Po	L	30	16 to 32 µm	24.3	8.02
		D	30	8 to 20 µm	14.33	6.02
	Uniporate conceptacles	D	3	174 to 400 µm	291.3	113.26
		H	3	71 to 140 µm	−	−
Neogoniolithon sp. (Fig. 4C)	VC	L	20	10 to 28 µm	19.6	6.5
		D	20	7 to 12 µm	9.2	1.7
	PF	L	50	9 to 20 µm	14.4	4.3
		D	50	5 to 11 µm	9.4	2.4
	Uniporate conceptacles	D	3	550 to 600 µm	576.6	20.75
		H	3	200 to 300 µm	250	40.82
Spongites fruticulosus Kützing, 1841 (Fig. 4D, E)	VC	L	50	16 to 24 µm	19.4	2.6
		D	50	12 to 18 µm	15	2
	PF	L	100	12 to 22 µm	16.4	3.9
		D	100	8 to 18 µm	12.6	3.5
	Epithallial cells	L	6	5 to 7 µm	5.8	0.74
		D	6	8 to 14 µm	10.6	2.15
Titanoderma pustulatum (Lamouroux) Nägeli, 1858 (Fig. 4F)	VC	L	20	12 to 18 µm	15	2
		D	20	8 to 15 µm	12	3.8
	PF	L	50	7 to 18 µm	12.6	3.8
		D	50	8 to 16 µm	11.2	2.9
	Uniporate conceptacles	D	17	110 to 140 µm	125	10
		H	17	72 to 94 µm	83.8	7.9
Amphiroa sp. (Fig. 4G-J)	Core region (long cells)	L	200 to 400	50 to 90 µm	66.6	17.25
		D	200 to 400	8 to 20 µm	12.8	4.2
	Core region (short cells)	L	60 to 80	16 to 40 µm	24.8	8.9
		D	60 to 80	9 to 19 µm	14.2	3.6
	Intergenicula	L	12 to 20	651 to 1109 µm	920	195
		D	12 to 20	256 to 338 µm	298	33.5
Corallina sp. (Fig. 5A-C)	Core region	L	105 to 245	18 to 24 µm	21.2	2.1
		D	105 to 245	8 to 12 µm	10	1.4

Table 1. — Continuation.

Taxa	Features/ Characteristics	Dimensions	Number of measuments (n)	Range	Mean (M)	Standard Deviation (SD)
	Intergenicula	L	7 to 35	350 to 1092µm	647.33	330
		D	7 to 35	134 to180 µm	154.6	19.07
Sporolithon cf. *airoldii* (Fig. 5D)	VC	L	25	8 to 16 µm	11.4	2.6
		D	25	3 to 8 µm	5.4	1.85
	PF	L	50	5 to 12 µm	9.4	2.5
		D	50	4 to 10 µm	7.6	2.2
	Sporangial compartments	L	70	80 to 120 µm	101	14.9
		D	70	35 to 48 µm	41.4	4.58
Sporolithon praeerythraeum (Airoldi) Vannucci, Piazza, Fravega & Basso, 2000 (Fig. 5E, F)	PF	L	50	14 to 26 µm	18.6	4.2
		D	50	10 to 12 µm	10.96	0.68
	Sporangial compartments	L	15	30 to 36 µm	32.3	2.1
		D	15	59 to 68 µm	61	10

Genus *Amphiroa* Lamouroux, 1812

Amphiroa sp.
(Fig. 4G-J)

DESCRIPTION

The intergenicular segments measure 651 to 1109 µm in length and 256 to 338 µm in diameter. Core region is composed of 3 to 6 layers of long cells alternating with 1 to 2 layers of short cells. Peripheral region not observed. Long cells measure 50 to 90 µm in length and 8 to 20 µm in diameter, short cells are 16 to 40 µm in length and 9 to 19 µm in diameter. Conceptacles are not preserved (Table 1).

REMARKS

The species of *Amphiroa* described herein is comparable to *Amphiroa fragilissima* (Linnaeus) Lamouroux illustrated by Johnson (1957) from the Pleistocene of Mariana limestone, Saipan. The characteristic features of *A. fragilissima* as defined by Johnson (1957) are the core region comprises of 3 to 6 layers of long cells alternating with 1 to 2 layers of short cells. However, the specimens described here show larger size of both long and short cells are. Moreover, owing to lack of preservation of conceptacles, the presently described form is not assignable to any known species of the genus.

Family CORALLINACEAE Lamouroux, 1812
Subfamily CORALLINOIDEAE Foslie, 1908
Genus *Corallina* Linnaeus, 1758

Corallina sp.
(Fig. 5A-C)

DESCRIPTION

Intergenicula cylindrical, measuring 350 to 1092 µm in length and 134 to180 µm in diameter. The rows of cells in the core region are rectangular in shape and measure 18 to 24 µm in length and 8 to 12 µm in diameter. Cell fusions are prominent (Table 1).

REMARKS

Based on the diagnostic features, the form is assignable to the genus *Corallina*. However, owing to lack of preservation of adequate taxonomic characteristics it is not possible to assign it to any known species of the genus. Different species of *Corallina* have been reported earlier from the Miocene of Kutch Basin, India (Kundal & Humane 2003).

Order SPOROLITHALES Le Gall, Payri, Bittner & Saunders, 2009
Family SPOROLITHACEAE Verheij, 1993
Subfamily SPOROLITHOIDEAE Setchell, 1943
Genus *Sporolithon* Heydrich, 1897

Sporolithon cf. *airoldii*
(Fig. 5D)

DESCRIPTION

Encrusting to warty growth form, thallus monomerous, dorsiventral, non-coaxial VC. The cells of VC are rectangular in shape that measure 8 to 16 µm in length and 3 to 8 µm in diameter. Cells of PF are more or less squarish with no distinct zonation, 5 to 12 µm in length and 4 to 10 µm in diameter. Cell fusions present. Epithallial cells and trichocytes are indiscernible. Sporangia elliptical, formed within calcified compartments and grouped into sori. Each sporangium measures 80 to 120 µm in height and 35 to 48 µm in diameter (Table 1).

REMARKS

The specimen is comparable to *Sporolithon airoldii* described from the lower Oligocene of NW Iran (Basso *et al.* 2019) in having small size of the vegetative cells and other anatomical features, but the maximum length of the sporangia exceeds that of the specimens described by Basso *et al.* (2019) as well as the type material of *S. airoldii*. Vannucci *et al.* (2010) re-described *S. airoldii* from the upper Rupelian-Chattian of Sassello while re-assessing Airoldi's (1932) specimens.
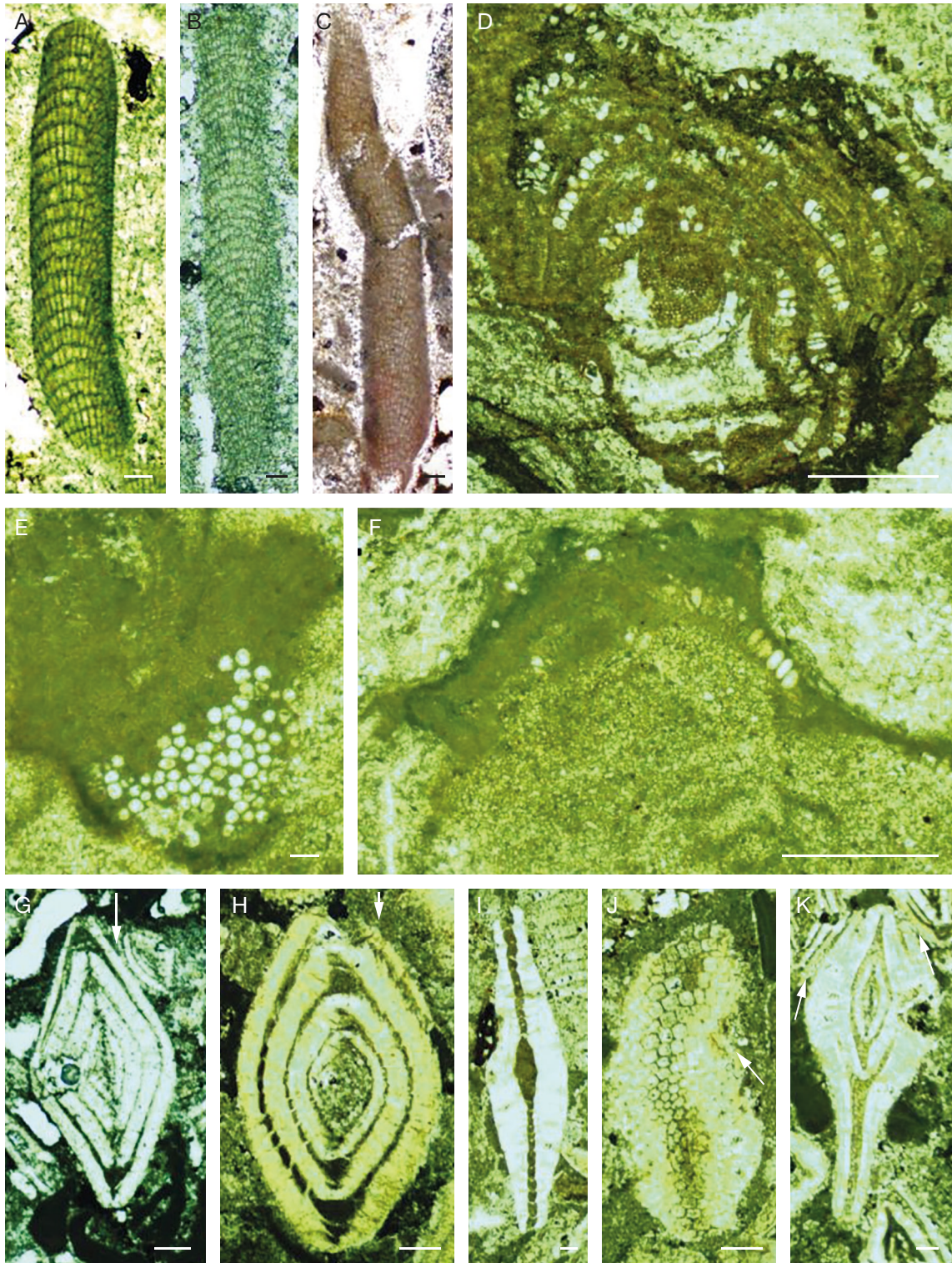
FIG. 5. — **A-C**, *Corallina* sp. (BSIP Slide No. 17036, 17027, 17030); **D**, *Sporolithon* cf. *airoldii* (BSIP Slide No. 17039) encrusting to warty growth form, thallus monomerous, cell fusions present, sporangia elliptical and grouped into sori; **E, F**, *Sporolithon praeerythraeum* (Airoldi) Vannucci, Piazza, Fravega & Basso, 2000 (BSIP Slide No. 17041) lumpy to protuberant growth form, cell fusions present in PF, sporangia grouped into sori; **G, H**, *Amphistegina* sp. (BSIP Slide No. 17033, 17037); **I, J**, *Cycloclypeus* sp. (BSIP Slide No. 17034, 17035); **K**, *Heterostegina* sp. (BSIP Slide No. 17036). **Arrows**: G, H, J, K, indicate compaction. Scale bars: A-C, 50 µm; D, F, 500 µm; E, I, K, 100 µm; G, H, J, 200 µm.
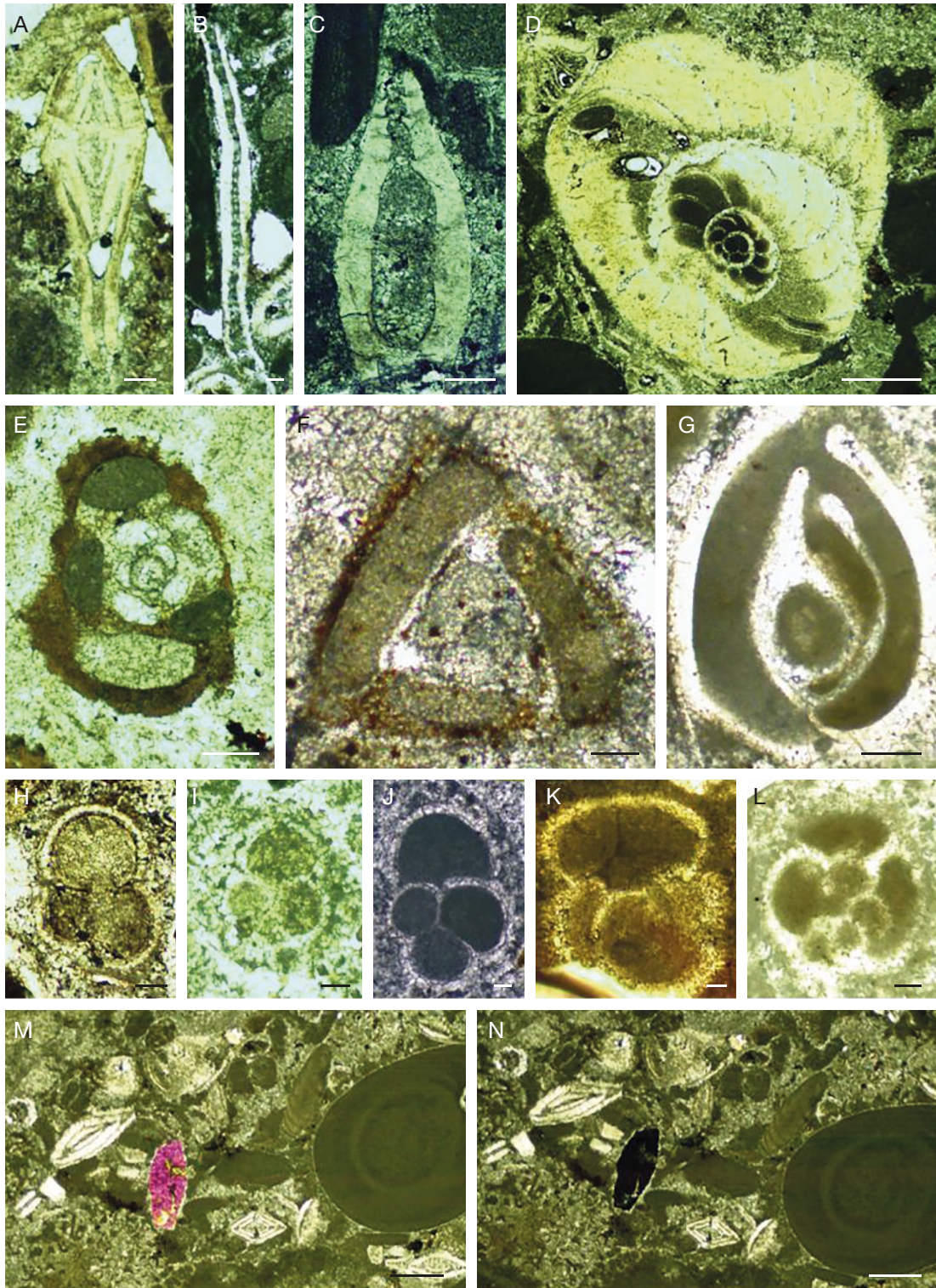
FIG. 6. — **A**, **B**, *Heterostegina* sp. (BSIP Slide No. 17037, 17033); **C**, unidentified nummulitid (BSIP Slide No. 17033); **D**, *Operculina* sp. (BSIP Slide No. 17038); **E**, *Quinqueloculina* sp. (BSIP Slide No. 17040); **F**, *Triloculina* sp. (BSIP Slide No. 17013); **G**, *Biloculina* sp. (BSIP Slide No. 17013); **H-J**, *Globigerinoides* sp. (BSIP Slide No. 17023); **K**, **L**, *Dentoglobigerina* sp. (BSIP Slide No. 17013); **M**, **N**, thin sections showing petrographic features. Scale bars: A, F, H-L, 50 µm; B, C, E, G, 100 µm; D, M, N, 500 µm;

TABLE 2. — Distribution of the species of coralline red algae from the studied outcrops (only the coralline red algae identified to the species level have been taken into consideration).

Taxa	Geographical distribution	Geological age	References
Mesophyllum roveretoi Conti, 1943	Tertiary Piedmont Basin	Upper Eocene to the Miocene	Fravega *et al.* (1987)
	Northern Croatia	Miocene	Basso *et al.* (2008)
	Leitha Limestone (Vienna Basin)	Badenian	Conti (1946)
Spongites fruticulosus Kützing, 1841	Gârbova de Sus Formation, Transylvanian Basin, Romania	Middle Miocene	Chelaru & Bucur (2016)
	Western and eastern Mediterranean Sea, NE Atlantic Ocean, Indian Ocean (Red Sea), Pacific Ocean (southern Australia)	Recent	Basso & Rodondi (2006)
	NW Italy	Miocene	Vannucci *et al.* (1994)
Lithoporella melobesioides (Foslie) Foslie, 1909	Austrian Molasse	Late Eocene	Rasser & Piller (1999)
	Northeast India	Late Eocene	Sarma *et al.* (2014)
	Southwest of Zaros Basin, Iran	Oligo-Miocene	Roozpeykar & Moghaddam (2016)
	Saurashtra, India	Pleistocene	Kundal *et al.* (2011)
	Tahiti, Japan	Pleistocene	Iryu *et al.* (2010)
	Agatti Island, Lakshadweep, India	Holocene	Misra *et al.* (2016)
	Reefs of Indo-Pacific region	Recent	Iryu *et al.* (2010)
Titanoderma pustulatum (Lamouroux) Nägeli, 1858	Iran	Early Oligocene	Bassi *et al.* (2019)
	United Kindom	Recent	Bailey (1999)
Sporolithon praeerythraeum (Airoldi) Vannucci, Piazza, Fravega & Basso, 2000	Gârbova de Sus Formation, Transylvanian Basin, Romania	Middle Miocene	Chelaru & Bucur (2016)
	Italy and Bulgaria	Late Eocene to early Oligocene	Francavilla *et al.* (1970); Bakalova (1983)

Sporolithon airoldii was recorded earlier from the Oligocene of Molare Formation of the Tertiary Piedmont Basin, NW Italy (Vannucci *et al.* 2010), from the lower and middle Rupelian of Prasco and Ovrano, Alessandria (Mastrorilli 1968), Val Lemme, Carrosio, Alessandria (Fravega *et al.* 1988), from the upper Rupelian to Chattian of Sassello, Savona (Airoldi 1932; Fravega *et al.* 1987), from the upper Burdigalian to Serravallian of St. Florent, N. Corsica and Bonifacio, Cala de Labra, S. Corsica (Mastrorilli in Bellini & Mastrorilli 1975) and from the lower Oligocene of NW Iran (Basso *et al.* 2019).

Sporolithon praeerythraeum (Airoldi) Vannucci, Piazza, Fravega & Basso, 2000
(Fig. 5E, F)

Archaeolithothamnium praeerithraeum Airoldi, 1932: 63, pl. 9, fig. 2.

Sporolithon praeerythraeum (Airoldi) Vannucci, Piazza, Fravega & Basso, 2000: 193.

DESCRIPTION
Lumpy to protuberant thallus, VC filaments indiscernible. The peripheral filaments (PF) show horizontal layers of elliptical cells. Cell fusions are present in the PF, the cells of PF measure 14 to 26 µm in length and 10 to 12 µm in diameter. Sporangia grouped in sori, individual sporangia measuring 30 to 36 µm in diameter and 59 to 68 µm in height (Table 1).

REMARKS
Vannucci *et al.* (2000) revised and re-documented this species of *Sporolithon* and transferred Airoldi's (1932) *Archaeo-*

lithothamnium praeerythraeum under the genus *Sporolithon* with a new combination. The species has been identified from the late Eocene to early Oligocene of Italy and Bulgaria (Francavilla *et al.* 1970; Bakalova 1983). The overall thallus organization, shape and size of the sporangia and the arrangement of the sporangia are closely comparable to the middle Miocene specimens recorded by Vannucci *et al.* (2000) and Chelaru & Bucur (2016).

BENTHIC AND PLANKTONIC FORAMINIFERS
In addition to the above mentioned coralline red algae, some benthic and planktonic foraminifers are also present, but owing to their poor preservation they are identifiable only up to generic level. The commonly occurring benthic foraminifers are represented by *Amphistegina* sp. (Fig. 5G, H), *Cycloclypeus* sp. (Fig. 5I, J), *Heterostegina* sp. (Figs 5K; 6A, B), unidentified nummulitids (Fig. 6C), *Operculina* sp. (Fig. 6D), *Quinqueloculina* sp. (Fig. 6E), *Triloculina* sp. (Fig. 6F), *Biloculina* sp. (Fig. 6G). The planktonic foraminifers are indeed difficult to identify in thin sections, however, on the basis of some distinguishing features some of them are identifiable up to genus level, namely *Globigerinoides* sp. (Fig. 6H-J), and *Dentoglobigerina* sp. (Fig. 6K, L).

FACIES AND SEDIMENTOLOGY
The different types of facies along with sedimentological features recognized in each outcrop are described as follows:

Butler Bay Section-I
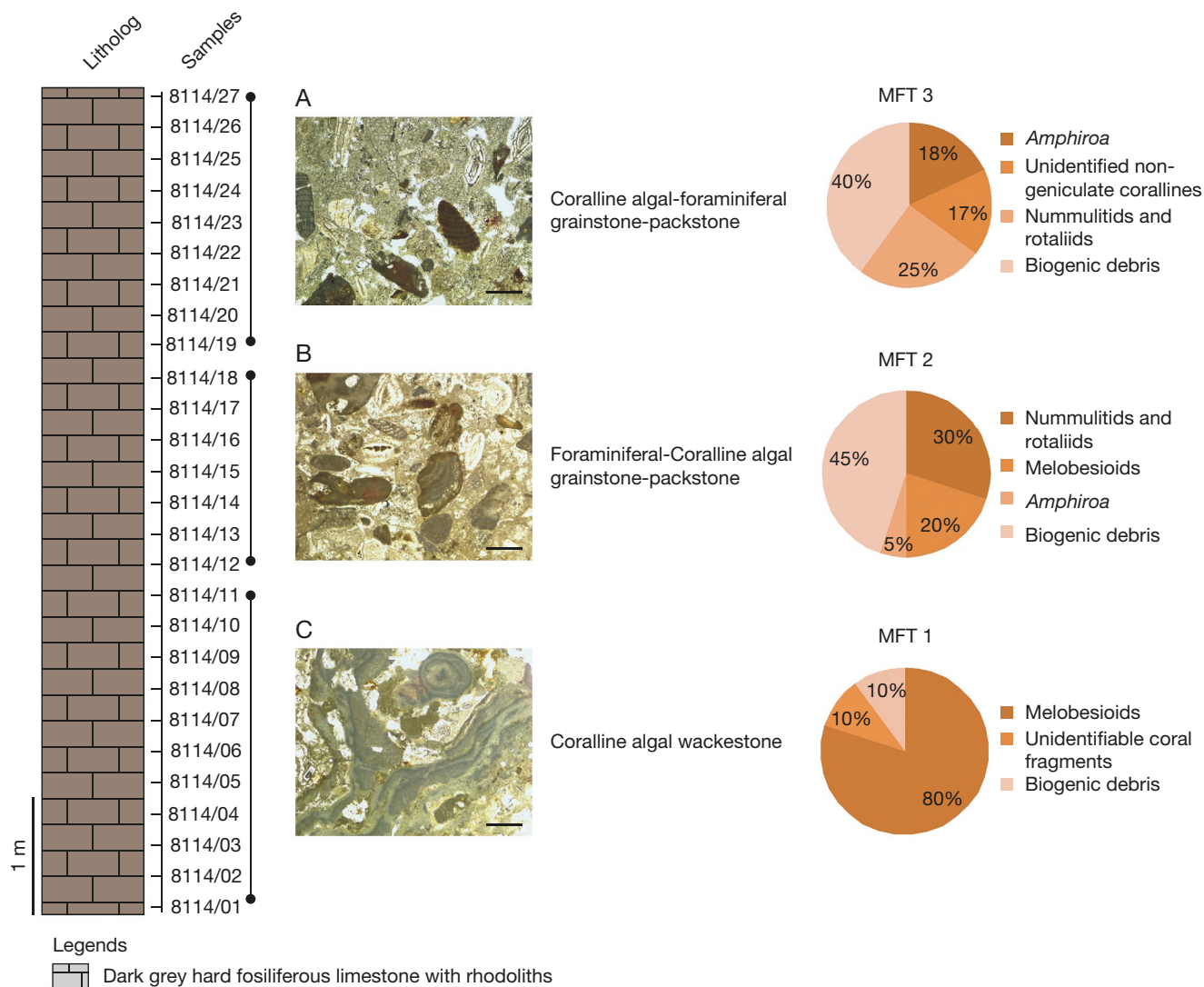MFT 1 Coralline algal wackestone (Sample no. 8114/01 to 8114/11, from base to 5.3 m; Fig. 7).

Fɪɢ. 7. — Types of facies with graphical representation from Butler Bay Section-I. Scale bars: A-C 500 µm.

The texture of this facies is mud-supported wackestone dominated by the rhodolith forming non-geniculate corallines such as melobesioids (80%). Subordinate components are unidentifiable coral fragments (10%) and biogenic debris (10%).

MFT 2 Foraminiferal-Coralline algal grainstone-packstone (Sample no. 8114/12 to 8114/18, from 5.3 to 9.08 m; Fig. 7)

This facies is characterized by poorly sorted grainstone to packstone with biogenic components dominated by the benthic foraminiferal genera belonging to Nummulitidae and rotaliids (30%). The non-geniculate coralline association is dominated by melobesioids (20 %) and the geniculate corallines represented by *Amphiroa* (5%) with other biogenic debris (45%).

MFT 3 Coralline algal-foraminiferal grainstone-packstone (Sample no. 8114/19 to 8114/27 from 9.08 to 14.48 m; Fig. 7)

This facies is characterized by poorly sorted grainstone to packstone, dominated by geniculate corallines mainly *Amphiroa* (18%), unidentified non-geniculate corallines (17%) Nummulitidae and rotaliids (25%) along with other biogenic debris (45%). Effects of fragmentation, disarticulation and abrasion are clearly visible in the coralline algae.

Butler Bay Section-II

MFT 1 Foraminiferal packstone (Sample no. 8898/01 to 8114/09, from base to 1.6 m; Fig. 8).

This facies consists of densely packed, poor to moderately sorted packstone with Nummulitidae (45%). Fragments of non-geniculate coralline algae of sub family Melobesioideae (20%) and coral fragments are also present in minor quantities. High rates of fragmentation, disarticulation and abrasion are observed in the coralline algae. Echinoid spines (5%) and other biogenic debris (30%) are also present.

MFT 2 Coralline algal-foraminiferal grainstone-packstone (Sample no. 8898/10 to 8114/16, from 1.6 to 3.35 m; Fig. 8).

This grainstone-packstone facies is composed of poor to moderately preserved melobesioids (30%) and unidentified geniculate coralline algae (20%) and benthic foraminifers, especially Nummulitidae and rotaliids (20%) associated with unidentified coral fragments (5%) and biogenic debris (25%). Disarticulation in geniculate corallines is common.

MFT 3 Foraminiferal-Coralline algal grainstone-packstone (Sample no. 8898/17 to 8114/20, from 3.35 to 4.35 m; Fig. 8).
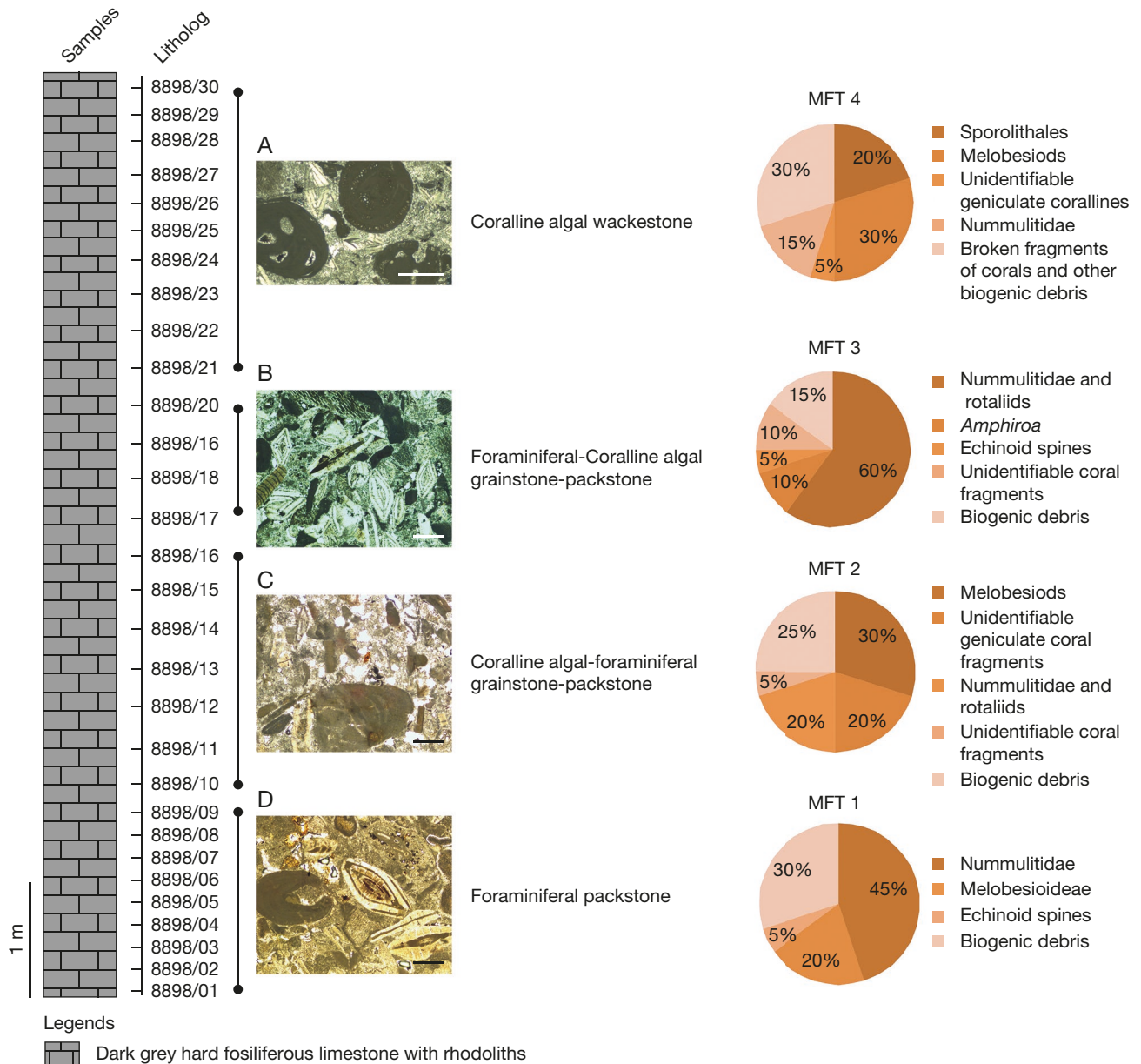
Fig. 8. — Types of facies with graphical representation from Butler Bay Section-II. Scale bars: A, 1 mm; B-D, 500 µm.

Both benthic foraminifers and coralline algae are present but the former is preponderant. Nummulitidae and rotaliids are dominant (60%), geniculate coralline algae *Amphiroa* (10%), echinoid spines (5%), unidentified coral fragments (10%) and biogenic debris (15%) are also present. Sparse grains of sparry calcite occur (Fig. 6M, N).

MFT4 Coralline algal-foraminiferal grainstone-packstone (Sample no. 8898/21 to 8114/30, from 4.35 to 6.85 m; Fig. 8).

This grainstone-packstone facies is composed of coralline algae represented by Sporolithales (20%) and melobesiods (30%), unidentifiable geniculate corallines (5%). Small Nummulitidae (15%) are also associated with the broken fragments of corals and other biogenic debris (30%).

Hut Bay Quarry No. 4 Section
MFT 1 Coralline algal wackestone (Sample no. 8900/01 to 8900/02 from base to 2 m; Fig. 9).

The texture of the facies is a mud-supported wackestone. This facies consists of large non-geniculate coralline algal thalli, especially of melobesiods (50%) and fragments of geniculate coralline algae *Amphiroa* (20%) and biogenic debris (30%). Both planktonic and benthic foraminifers are absent.

MFT 2 Foraminiferal-Coralline algal wackestone (Sample no. 8900/03, from 2 to 4 m; Fig. 9).

This facies is also characterized by mud-supported wackestone. A major change in this facies have been noticed from the previous one, due to the appearance of large benthic foraminifers, especially Nummulitidae (30%) with subordi-
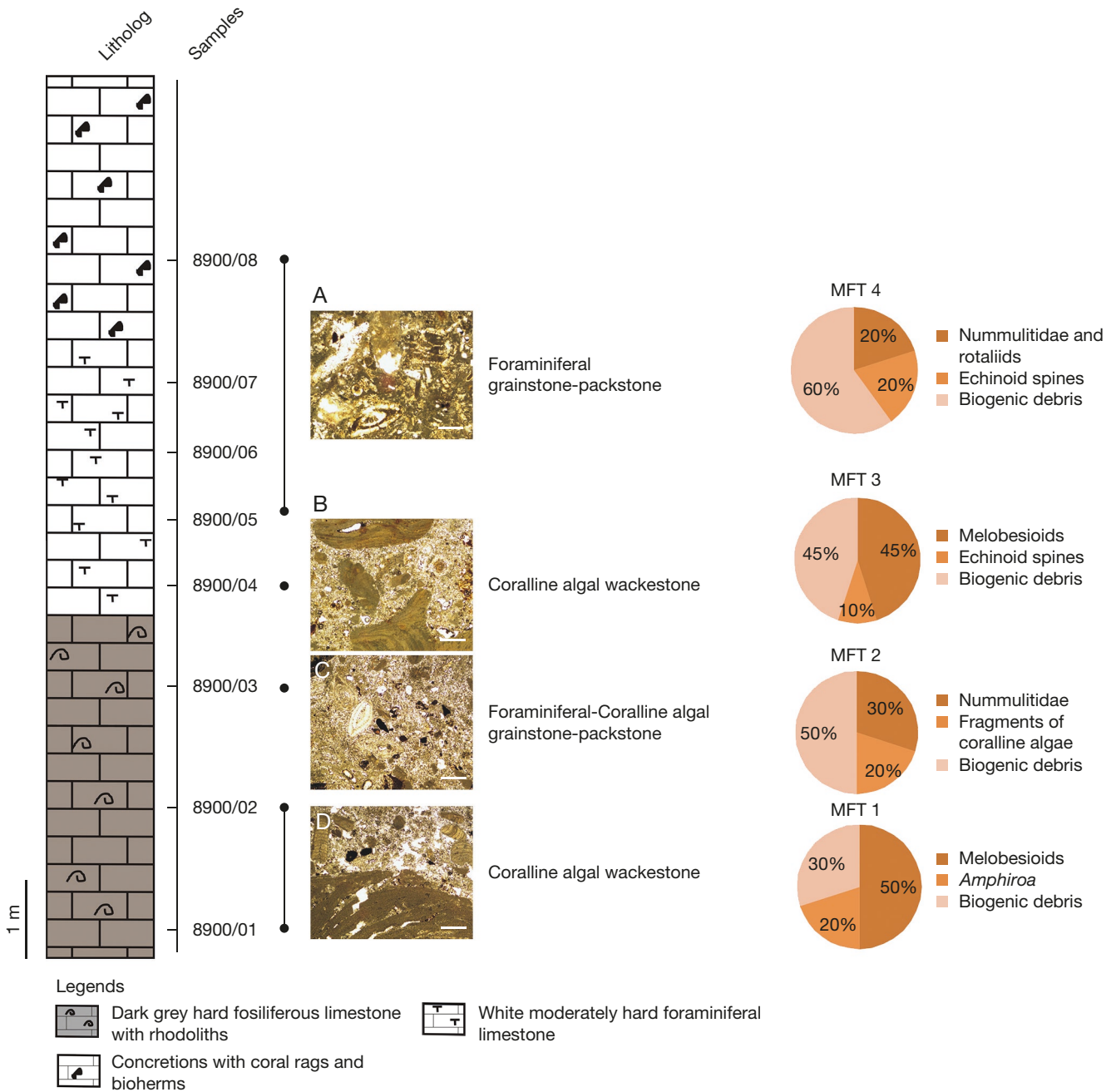
Fɪɢ. 9. — Types of facies with graphical representation from Hut Bay Quarry No. 4 Section. Scale bars: A-D, 500 μm.

nate components represented by fragments of coralline algae (20%) and biogenic debris (50%). Due to severe abrasion, the algal forms are difficult to identify even up to generic level.

MFT 3 Coralline algal wackestone (Sample no. 8900/04, from 4 to 4.88 m; Fig. 9).

Large coralline algal thalli in a mud supported wackestone characterize this facies. High rates of fragmentation, disarticulation and abrasion are observed in the geniculate coralline algae and non-geniculate melobesiods (45%). Some echinoid spines are also present in minor quantities (10%) along with biogenic debris (45%).

MFT 4 Foraminiferal grainstone-packstone (Sample no. 8900/05 to 8900/08, from 4.88 to 10.52 m; Fig. 9).

Poor to moderately preserved larger benthic foraminifers are abundant in this grainstone-packstone facies. Abundance of rotaliids and taxa belonging to Nummulitidae (20%) has been observed along with echinoid spines (20%) and biogenic debris (60%). This facies is devoid of coralline algae.

New Quarry Section
MFT 1 Coralline algal-foraminiferal grainstone-packstone (Sample no. 8901/01 to 8901/04, from base to 9.9 m; Fig. 10).

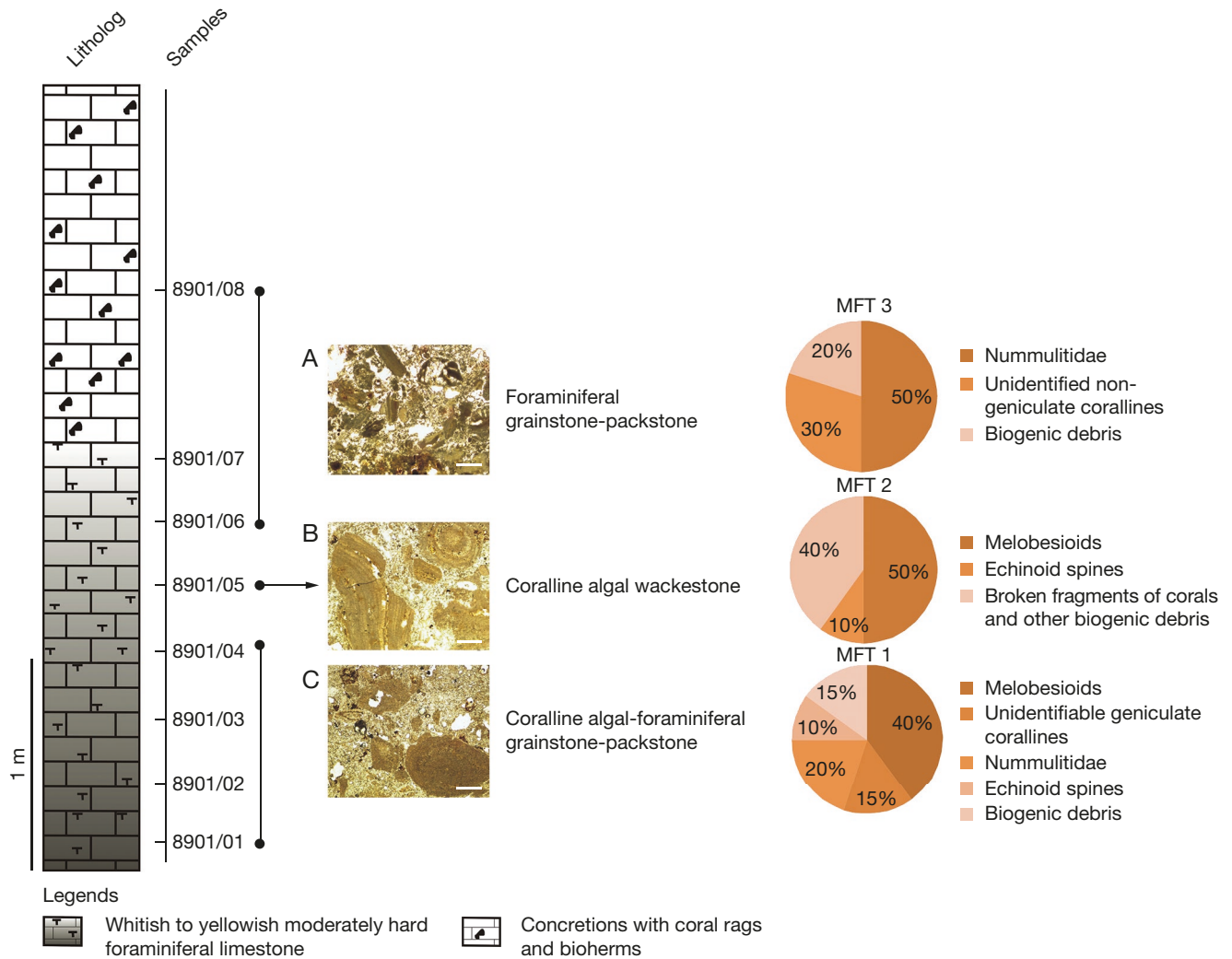FIG. 10. — Types of facies with graphical representation from New Quarry Section. Scale bars: A-C, 500 µm.

This grainstone-packstone facies is dominated by non-geniculate melobesioids (40%), unidentified geniculate corallines (15%) along with Nummulitidae foraminifers (20%), echinoid spines (10%) and broken fragments of corals and other biogenic debris (40%). The overall texture is a poorly sorted grainstone-packstone.

MFT 2 Coralline algal wackestone (Sample no. 8901/05, from 9.9 to 1.32 m; Fig. 10).

A moderately sorted wackestone, rich in melobesiods (50%) in association with echinoids (10%) and broken fragments of corals and other biogenic debris (40%).

MFT 3 Foraminiferal grainstone-packstone (Sample no. 8901/06 to 8901/08, from 1.32 to 3.48 m; Fig. 10).

This facies is characterized by poorly sorted grainstone-packstone, dominated by foraminifers, especially Nummulitidae (50%) and unidentifiable geniculate coralline algae (30%) and other biogenic debris (20%).

CORALLINE GROWTH FORM AND RHODOLITH MORPHOTYPES
Various types of growth forms in coralline algae have been encountered in the present study such as encrusting (Figs 3A-D;

4A, B, F), or protuberant (Figs 5D; 11E, F), foliose (Fig. 3C), layered lamellae (Fig. 3A, B) and arborescent (Figs 4G-J; 5A-C). Corallines formed rhodoliths 30-50 mm in diameter, with irregular to ellipsoidal shapes and a boxwork morphotype (Basso 1998) (Fig. 11A-D). The boxwork rhodoliths (Fig. 11A-D) have laminar concentric to columnar internal structure (Bosence 1983b; Basso 1998) and are dominated by *Mesophyllum* sp. (Fig. 3E)*, Mesophyllum roveretoi* (Fig. 3F) and ?*Lithothamnion valens* (Fig. 3A, B). The commonly occurring rhodolith-forming algae are *Lithoporella melobesiodies* (Fosile) Foslie, 1909 (Fig. 4A, B) and *Sporolithon* cf. *airoldii* (Fig. 5D). In addition, some algal taxa are rarely represented in the rhodoliths, e.g. *Phymatolithon* sp. (Fig. 3C, D)*, Spongites fruticulosus* (Fig. 4D, E)*, Titanoderma pustulatum* (Fig. 4F)*, Sporolithon praeerythraeum* (Fig. 5E, F) and *Neogoniolithon* sp. (Fig. 4C). Boxwork morphotypes show numerous macroscopic voids which are occupied with sediments.

TAPHONOMIC FEATURES
The taphonomic processes left an important overprint on the studied fossil assemblages. Based on the major biostratinomic
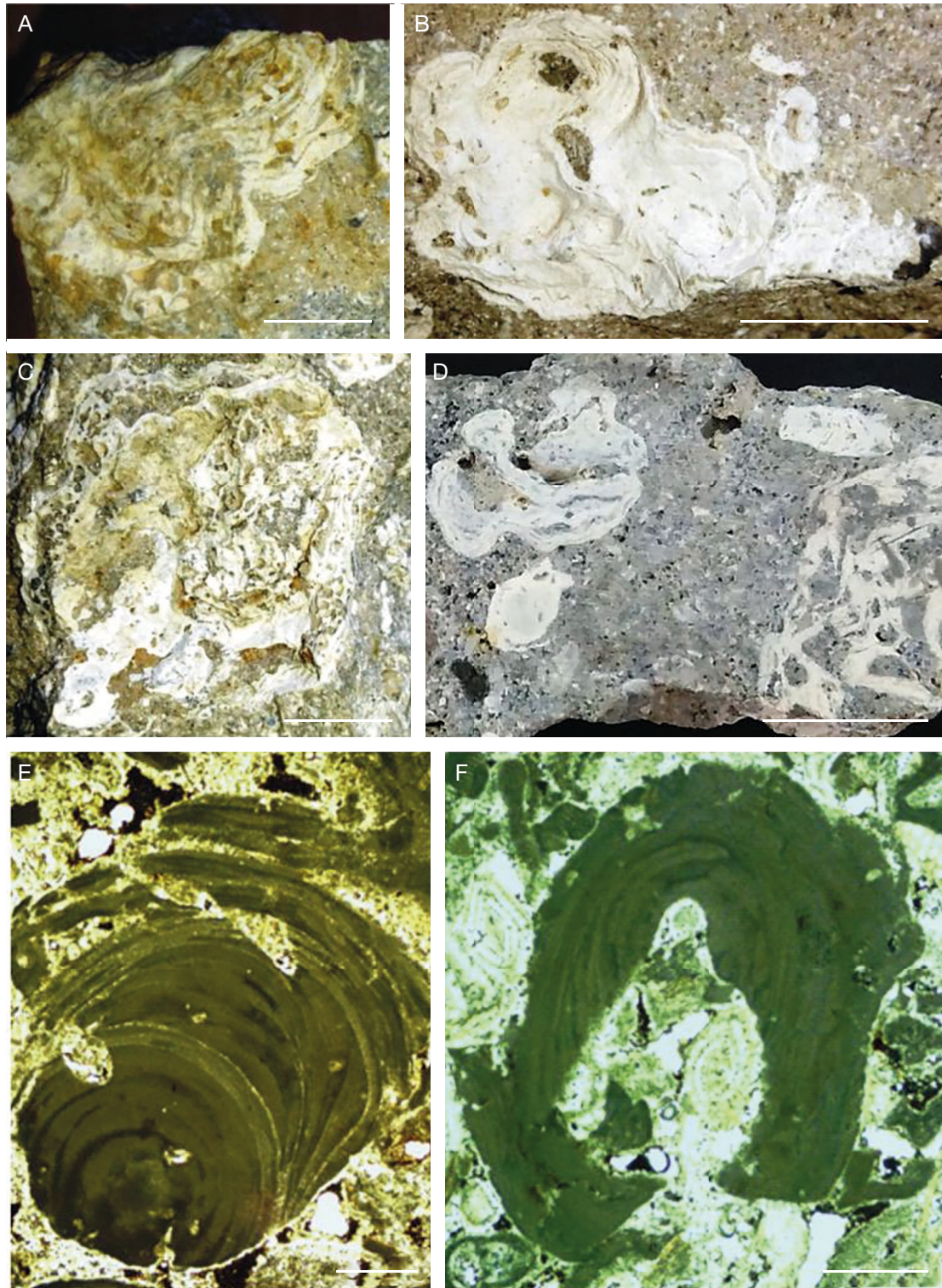
Fig. 11. — **A-D**, Polished surface of the sliced rock samples showing boxwork laminar concentric rhodoliths; **E**, **F**, melobesiods (BSIP Slide No. 17040) showing abrasion (**E**) and bioerosion (**F**). Scale bars: A, C, 5 mm; B, D, 10 mm; E, F, 500 µm.

features in coralline algae and foraminifers, encrustation (Fig. 3A-D; 4A, B, F), abrasion (Fig. 11E, F), bioerosion (Figs 3E; 11F), and fragmentation (Figs 4I, J; 5C) (Nebelsick & Bassi 2000; Basso *et al.* 2009) have been envisaged. Moreover, geniculate species of *Amphiroa* (Fig. 4I, J) and *Corallina* (Fig. 5C) underwent disarticulation. Diagenetic alteration was observed in corallines and in both larger benthic and planktonic foraminifers. Micritization, cementation and compaction are some of the diagenetic signatures that have been identified. The diagenetic micritization has been detected as a dark rim surrounding the skeletal grains of some benthic foraminifers such as *Quinqueloculina* sp. and

Triloculina sp. (Fig. 6E, F). Fine crystalline rim cement around the planktonic foraminifers has been observed that may also be due to diagenesis (Fig. 6H-L). Compaction of bioclastic carbonate sand occurred both mechanically and chemically (Croizé *et al.* 2010). Sediment progressively loses its porosity by compaction due to the effects of pressure from loading. In our material, compaction has been detected as low porosity and contact of grains. In case of mechanical compaction both point contact (Fig. 6C) and tangential contact (Figs 5G, H, K; 6B) are clearly discernible. Partial chemical dissolution is apparent in the poor preservation of finest details of coralline algae (Fig. 3B-D; 4A-C, F) and the effect of consequent compaction, one of the important diagenetic processes in a burial environment, has been observed in benthic foraminifera, such as *Cycloclypeus* sp. (Fig. 5J). The compaction might have occurred after diffused chemical dissolution that also affected the preservation potential of coralline red algae.

DISCUSSION

Facies characterization of the carbonate sediments of the Long Formation on Little Andaman Island has been assessed to interpret the paleoenvironment. On the basis of biogenic composition and depositional fabric three facies types have been demarcated in the Butler Bay Section-I (Fig. 7), four facies types have been recognized in Butler Bay Section-II (Fig. 8), four facies have been identified in Hut Bay Quarry No.4 (Fig. 9) and three different facies have been recognized in the New Quarry Section (Fig. 10). As far as biogenic composition and depositional fabric of the carbonate sediments are concerned, all the four outcrops are characterized by more or less same features with minor alternation and variation.

It is well established that rhodoliths occur in carbonate or mixed siliciclastic deposits from the intertidal down to *c.* 200 m water depth, and are globally distributed from the equator to circumpolar latitudes (Foster 2001; Riosmena-Rodríguez *et al.* 2017; Rebelo *et al.* 2021). Although there are many published records on the rhodolith facies from the Paleogene (Manker & Carter 1987; Rasser & Piller 2004), they became more abundant during the Neogene (Halfar & Mutti 2005). In the Miocene, coralline algae and rhodoliths were at their acme and they more or less replaced the coral-reefs, which was associated with the decline of other carbonate-producing phototrophs (Halfar & Mutti 2005; Pomar *et al.* 2017). The Miocene rhodoliths accumulated in the Tethys and Paratethys regions as well as in a number of localities in the tropical Pacific, Southeast Asia, and the Caribbean regions (Halfar & Mutti 2005). Coralline algae and rhodoliths were dominant in the circum-Mediterranean region during Burdigalian to Serravallian (Esteban 1996). Abundant occurrences of rhodalgal carbonates during late Burdigalian to the early Serravallian are synchronous with the Monterey event (Halfar & Mutti 2005; Braga 2017; Pomar *et al.* 2017). This event is defined by a prominent and long-lasting phase of the middle Miocene (17.5-13.5 Ma) carbon-isotope excursion represented by the higher δ¹³C values known as the Middle-Miocene Climatic Optimum (MMCO). The dominance of rhodalgal facies over coral-reef carbonates can be correlated to the carbon-isotope excursion (Halfar & Mutti 2005; Pomar *et al.* 2017). Therefore, the dominance of coralline algae in the studied sections of Little Andaman Island (Hut Bay) which has been dated earlier based on planktonic foraminifers (Srinivasan 1988; Sharma & Srinivasan 2007) may be correlated with the terminal phase of the MMCO event. After the MMCO event the global temperature declined, along with a decrease of the carbonate content and mass accumulation rate in the paleoceanographic record of the Equatorial Indian Ocean (Lübbers *et al.* 2019) that was accompanied by an intertropical belt contraction and the consequent reduction of the distribution of some tropical coralline genera (Braga & Bassi 2007).

Various rhodolith forming red algal flora have been reported from the middle Miocene. Two main types of rhodolith-building coralline associations were reported by Martín *et al.* (1993) from the Marion Plateau (Northeastern Australia). The first type is composed of *Lithothamnion* and *Sporolithon* with subordinate representation of *Hydrolithon, Mesophyllum, Spongites,* and *Lithoporella*. The other type is principally made up of *Mesophyllum* and the present assemblage is to some extent comparable to this type in having dominance of *Mesophyllum.*

Since the time of their definition (Bosellini & Ginsburg 1971), it was suggested that rhodolith shape, growth form and inner algal arrangement provide significant information on the palaeoenvironment. Water energy is an important factor which controls the growth of rhodoliths in a particular environment (Bosence 1991; Basso 1998; Bracchi *et al.* 2022). Different types of rhodolith shapes have been proposed by Bosellini & Ginsburg (1971). Bosence (1991) opined that the rhodoliths composed of radially developed, twig-like branches generally inhabit in quieter environments where transportation of rhodoliths is minor. On the other hand, the densely branched forms and the pralines grow in higher energy conditions (Basso 1998; Sañé *et al.* 2016; Bracchi *et al.* 2022). Based on the present-day distribution of the various rhodolith morphologies and structures, it was proposed a simplified system for a rapid identification of the main rhodolith morphotypes, depending mainly on substrate stability/hydrodynamics and sedimentation rate (Basso 1998; Basso *et al.* 2009, 2016).

Different types of processes are involved in the development of fossil rhodolith beds such as growth forms, taphonomic filters, water energy, types of deposition, i.e., allochthonous or autochthonous (Bosence 1991; Aguirre *et al.* 2017). Important palaeoecological constraints can be derived from a combination of observations such as rhodolith morphotypes, taxonomic composition and succession of the coralline algae within the rhodoliths, morphology and growth forms of the algal thalli, internal arrangement of the rhodoliths, taphonomic signatures and interactions of organisms (Basso 1998; Basso *et al.* 1998; Nebelsick & Bassi 2000; Basso *et al.* 2009; Aguirre *et al.* 2017; Coletti *et al.* 2018).

In the present study, rhodoliths are present in all the sections and most of them are irregular to elliptical in shape.

The rhodolith morphotype is dominantly boxwork, with laminar concentric to columnar internal structure. This indicates a moderate to low hydrodynamics (Basso 1998). The rhodoliths are multispecific with abundant representation of melobesioids viz., *Mesophyllum* sp.*, Mesophyllum roveretoi* and ?*Lithothamnion valens*. The commonly occurring rhodolith-forming corallines are represented by *Lithoporella melobesiodies* and *Sporolithon* cf. *airoldii* (Fig. 5D). Some taxa rarely form rhodoliths, e.g. *Phymatolithon* sp., *Spongites fruticulosus, Titanoderma pustulatum, Sporolithon praeerythraeum* and *Neogoniolithon* sp.

Palaeobathymetry is one of the most important aspects that can be derived from the coralline algal assemblages, in addition to the hydrodynamic and palaeoclimatic conditions (Bosence 1983b, 1991; Aguirre *et al.* 2000; Braga & Aguirre 2001; Piller 2003; Coletti *et al.* 2018). In a recent study, Li *et al.* (2021) estimated the palaeobathymetry of several non-geniculate coralline genera in the northern South China Sea since the Pliocene. According to their estimation, the bathymetric range of the genera *Lithoporella, Lithothamnion, Mesophyllum, Spongites* and *Titanoderma* is intertidal to 25 m water depth. This conclusion is not supported by the worldwide distribution of the genera *Mesophyllum* and *Lithothamnion* that basically thrive below 20 m of water depth, even down to 100 m (Adey 1986; Braga & Aguirre 2004). However, Coletti & Basso (2020) reported the occurrence of both the genera from 20-40 m water depth. The distribution of modern species of *Lithothamnion* indicates that this genus occurs in deeper water than *Mesophyllum* (Adey 1986; Lund *et al.* 2000). Though the genus *Mesophyllum* has a wide depth distribution, its occurrence has been documented from 15 to 30 m water depth in the recent coralline algal assemblage of the Ryukyu Group, Japan (Iryu 1992), in the modern and Pleistocene coral reefs of eastern Australia (Lund *et al.* 2000; Braga & Aguirre 2004), and in the early Miocene of the Sommières Basin, Southern France (Coletti *et al.* 2018). The genus *Lithophyllum* is widely distributed and common in shallow waters, especially in the intertropical belt (Vieira-Pinto *et al.* 2014; Basso *et al.* 2015; Jesionek *et al.* 2016; Kato & Baba 2019). Though there is no record of depth distribution of *Spongites, Neogoniolithon* and *Phymatolithon* in the Indian Ocean, it has been suggested that *Spongites fruticulosa* is widespread in the present day Mediterranean Sea at a depth range of 12 to 75 m (Hrabovský *et al.* 2015). Mateo-Cid *et al.* (2014) reported the occurrence of *Neogoniolithon mamillare* in the Mexican Caribbean at a water depth ranging from intertidal to 30 m. The depth distribution of *Phymatolithon* is known from Namibia and Mozambique, spanning 8-14 m of water depth (Van Der Merwe & Maneveldt 2014). According to Minnery *et al.* (1985), sporolithaceans predominantly occur between 20 and 50 m water depth. Later, Rasser & Piller (1997) estimated that the genus *Sporolithon* is dominant between 20 and 40 m water depth, while Aguirre *et al.* (2000) opined that in the modern tropical ocean sporolithaceans are abundant between 40-50 m water depth. Very shallow occurrences of *Sporolithon* also have been recorded (Verheij 1993; Basso *et al.* 2009; Neill *et al.* 2015) and a poleward

emergence of the genus was postulated (Basso *et al.* 2009). Therefore, sporolithaceans are globally distributed both in shallow and moderately deep-water settings (Adey 1986), and no direct evidence in the geological record indicates that the sporolithaceans increase with increasing water depth (Fravega *et al.* 1989; Brandano *et al.* 2005, 2007; Braga *et al.* 2009; Coletti *et al.* 2018; Chelaru *et al.* 2019). However, the dominance of boxwork rhodoliths and the coralline assemblage do point to a fore slope paleoenvironment. This interpretation is also supported by the foraminifers association, including the occurrence of the deep water genus *Cycloclypeus* (Novak & Renema 2018) . In fact, on a global scale, geniculate coralline algae are more abundant in shallow water (*c.* 15 to to 20 m), while non-geniculate corallines are more frequently dominant in deeper water (Johansen 1974; Konar & Foster 1992).

Various taphonomic features have been visualized in thin section analysis, e.g. encrustation has been specifically noted in the non-geniculate corallines such as *Lithoporella, Neogoniolithon* and *Phymatolithon* (Figs 3; 4) etc. Disarticulation and fragmentation are common in geniculate corallines, e.g. *Amphiroa* (Fig. 9G-J) and *Corallina* (Fig. 5A-C), as expected for bioclasts produced in shallow water. Other taphonomic features such as abrasion (Fig. 11E), bioerosion (Figs 3E; 11F), chemical dissolution (Figs 3B, D; 4A, C, F), compaction (Fig. 6G, H, J, K) are also commonly observed. After deposition, the sediments undergo increase of temperature and pressure due to burial under successive younger layers. The evidence of diagenetic effect in carbonate sediments in the microscopic study of thin sections analysis is a common feature in larger benthic foraminifers. The common diagenetic effects identified are micritization, cementation and compaction. Due to micritization, changes in the original grain structure took place.

Studies have been carried out earlier on the reconstruction of the lost carbonate factories built by skeletal elements of coralline red algae and benthic foraminifers (Nebelsick *et al.* 2001; Rasser & Nebelsick 2003; Basso *et al.* 2012; Leszczyński *et al.* 2012; Coletti *et al.* 2015). These skeletal remains that were transported basinward could provide information on the original depositional environment. The coralline red algal assemblage along with benthic foraminifers recorded herein from the Serravallian sections of Little Andaman also provides substantial information on their depositional environment. Geniculate corallines, miliolids and coral rubble, together with evidence of fragmentation and abrasion, support the occurrence of a shallow-water platform with colonial z-corals, that was the source of the below wave base gravity deposits produced by storms, accumulated on a fore-reef slope. There, an in-situ biogenic production could still take place, adding to the transported sediment and explaining the occurrence of relatively deep-water coralline species and the formation of boxwork rhodoliths.

Though quantification of rhodolith density and mass accumulation rate is beyond the scope of the present study, our results indicate that carbonate production was still considerably high in the tropical northeast Indian Ocean during the Serravallian.

CONCLUSIONS

This is the first comprehensive record of rhodoliths from the Serravallian of tropical northeast Indian Ocean. The Serravallian age for the studied outcrops is based on the earlier study on index planktonic foraminifers (Srinivasan 1988; Sharma & Srinivasan 2007). Most of the rhodolith morphotypes are boxwork in nature with concentric to laminar internal structure that designate moderate to low energy settings. Owing to such hydrodynamic settings, various taphonomic signatures (encrustation, disarticulation, fragmentation, bioerosion, abrasion and diagenesis) were noted in the rhodolith forming coralline red algae. Diagenetic effects are represented by micritization, cementation and compaction. Geniculate coralline algae are also common in the studied thin sections, though they were not abundant and never observed within the rhodoliths. Most of the geniculates show fragmentation and disarticulation that also implies transport. The growth forms in non-geniculate corallines are represented by encrusting, warty, lumpy, layered and foliose, whereas in geniculate forms arborescent growth form is common. Different facies types were identified from the four sections, where most of them are wackestone and packstone which are characterized by algal-foraminiferal bioclastic limestone composed of coralline red algae, benthic and planktonic foraminifers, echinoid spines and coral fragments. The observed bioclastic associations suggest that most of the carbonate production occurred on a shallow-water high-energy platform, though exact bathymetric estimation is very much speculative. Gravity deposits occurred in a slope off-reef environment, with in situ formation of multispecific boxwork rhodoliths composed of deeper coralline species associated with planktonic foraminifers, the latter probably transported from offshore settings. The present study envisages that the carbonate production flourished during the Serravallian of tropical northeast Indian Ocean.

REFERENCES

ADEY W. H. 1986. — Coralline algae as indicators of sea-level, *in* VAN DE P. (ed.), *Sea-Level Research: A Manual for the Collection and Evaluation of Data.* Springer Dordrecht, Amsterdam: 229-280. https://doi.org/10.1007/978-94-009-4215-8_9

ADEY W. H. & MACINTYRE I. G. 1973. — Crustose coralline algae: A re-evaluation in the geological sciences. *Bulletin of the Geological Society of America* 84: 883-904. https://doi.org/10.1130/0016-7606(1973)84%3C883:C-CAARI%3E2.0.CO;2

AGUIRRE J. & BRAGA J. C. 1998. — Redescription of Lemoine's (1939) types of coralline algal species from Algeria. *Palaeontology* 41: 489-507. https://www.biodiversitylibrary.org/page/49739586

AGUIRRE J., RIDING R. & BRAGA J. C. 2000. — Diversity of coralline red algae: origination and extinction patterns from the Early Cretaceous to the Pleistocene. *Paleobiology* 26 (4): 651-667. https://doi.org/10.1666/0094-8373(2000)0262.0.CO;2

AGUIRRE J., BRAGA J. C., REVIERS B. & WOELKERLING W. J. 2012. — Reassessment of Lemoine's newly discovered types of fossil corallines (Corallinales, Rhodophyta) preserved at the Muséum national d'Histoire naturelle, Paris. *Cryptogamie, Algologie* 33 (3): 289-326. https://doi.org/10.7872/crya.v33.iss3.2012.289

AGUIRRE J., BRAGA J. C. & BASSI D. 2017. — Rhodoliths and rhodolith beds in the rock record, *in* RIOSMENA-RODRIGUEZ R., NELSON W. & AGUIRRE J. (eds), *Rhodolith/Maërl beds: A global perspective*. Springer, Cham: 105-138. https://doi.org/10.1007/978-3-319-29315-8_5

AIROLDI M. 1932. — Contributo allo studio delle Corallinacee del terziario italiano. I. Le Corallinacee dell'Oligocene ligure-piemontese, Pisa. *Paleontographia Italica* 33 (3): 55-83.

ATHANASIADIS A. 2016. — *Phycologia Europaea Rhodophyta*. Vol. I. Published and distributed by the author, Thessaloniki, 762 p.

BAILEY J. C. 1999. — Phylogenetic positions of *Lithophyllum incrustans* and *Titanoderma pustulatum* (Corallinaceae Rhodophyta) based on 18S rRNA gene sequence analyses, with a revised classification of the Lithophylloideae. *Phycologia* 38 (3): 208-216. https://doi.org/10.2216/i0031-8884-38-3-208.1

BAKALOVA D. 1983. — Paleogene calcareous algae of division Rhodophyta from the area of the town of Asenovgrad, South Bulgaria (in Bulgarian). *Paleontology, Stratigraphy and Lithology* 18: 43-68.

BARNES J., BELLAMY D. J., JONES D. J. & WHITTON B. A. 1970. — Sublittoral reef phenomena of Aldabra. *Nature* 225: 268-269. https://doi.org/10.1038/225268a0

BASSI D., BRAGA J. C., DI DOMENICO G., PIGNATTI J., ABRAMOVICH S., HALLOCK P., KÖNEN J., KOVÁCS Z., LANGER M. R., PAVIA G. & IRYU Y. 2019. — Palaeobiogeography and evolutionary patterns of the larger foraminifer *Borelis* de Montfort (Borelidae). *Papers in Palaeontology* 7 (1): 377-403. https://doi.org/10.1002/spp2.1273

BASSO D. 1998. — Deep rhodolith distribution in the Pontian Islands, Italy: A model for the paleoecology of a temperate sea. *Palaeogeography, Palaeoclimatology, Palaeoecology* 137 (1-2): 173-187. https://doi.org/10.1016/S0031-0182(97)00099-0

BASSO D. 2012. — Carbonate production by calcareous red algae and global change. *Geodiversitas* 34 (1): 13-33. https://doi.org/10.5252/g2012n1a2

BASSO D. & TOMASELLI V. 1994. — Palaeoecological potentiality of rhodoliths: A Mediterranean case history, *in* MATTEUCCI R., CARBONI M. G. & PIGNATTI J. S. (eds), *Studies on Ecology and Paleoecology of Benthic communities. Bollettino della Società Paleontologica Italiana* Special volume 2: 17-27.

Basso D. & Rodondi G. 2006. — A Mediterranean population of *Spongites fruticulosus* (Rhodophyta, Corallinales), the type species of *Spongites*, and the taxonomic status of *S. stalactitica* and *S. racemosa,* Lawrence. *Phycologia* 45 (4): 403-416. https://doi.org/10.2216/04-93.1

Basso D., Fravega P. & Vannucci G. 1997. — The taxonomy of *Lithothamnium ramosissimum* (GÜMBEL non REUSS) CONTI and *Lithothamnium operculatum* (Conti) Conti (Rhodophyta, Corallinaceae). *Facies Erlangen* 37: 167-182. https://doi.org/10.1007/BF02537377

Basso D., Fravega P., Piazza M. & Vannucci G. 1998. — Revision and re-documentation of M. Airoldi's species of *Mesophyllum* from the Tertiary Piedmont Basin (NW Italy). *Rivista Italiana di Paleontologia e Stratigrafia* 104 (1): 85-94. https://doi.org/10.13130/2039-4942/6117

Basso D., Vrsaljko D. & Grgasović T. 2008. — The coralline flora of a Miocene maërl: the Croatian "Litavac". *Geologica Croatica* 61 (2-3): 333-340. https://doi.org/10.4154/GC.2008.25

Basso D., Nalin R. & Nelson C. S. 2009. — Shallow-water *Sporolithon* rhodoliths from North Island (New Zealand). *Palaios* 24 (2): 92-103. https://doi.org/10.2110/palo.2008.p08-048r

Basso D., Quaranta F., Vannucci G. & Piazza M. 2012. — Quantification of the coralline carbonate from a Serravallian rhodolith bed of the Tertiary Piedmont Basin (Stazzano, Alessandria, NW Italy). *Geodiversitas* 34 (1): 137-149. https://doi.org/10.5252/g2012n1a8

Basso D., Caragnano A., Le Gall L. & Rodondi G. 2015. — The genus *Lithophyllum* in the north-western Indian Ocean, with description of *L. yemenense* sp. nov., *L. socotraense* sp. nov., *L. subplicatum* comb. et stat. nov., and the resumed *L. affine*, *L. kaiseri*, and *L. subreduncum* (Rhodophyta, Corallinales). *Phytotaxa* 208 (3): 183-200. https://doi.org/10.11646/phytotaxa.208.3.1

Basso D., Babbini L., Kaleb S., Bracchi V. A. & Falace A. 2016. — Monitoring deep Mediterranean rhodolith beds. *Aquatic Conservation: Marine and Freshwater Ecosystems* 26 (3): 549-561. https://doi.org/10.1002/aqc.2586

Basso D., Babbini L., Ramos-Esplá A. A. & Salomidi M. 2017. — Mediterranean rhodolith beds, *in* Riosmena-Rodriguez R., Nelson W. & Aguirre J. (eds), *Rhodolith/Maërl Beds: a global perspective*. Springer, Cham: 281-298. https://doi.org/10.1007/978-3-319-29315-8_11

Basso D., Coletti G., Bracchi V. A. & Yazdi-Moghadam M. 2019. — Lower Oligocene coralline algae of the Uromieh section (Qom Formation, NW Iran) and the oldest record of *Titanoderma pustulatum* (Corallinophycidae, Rhodophyta). *Rivista Italiana di Paleontologia e Stratigrafia* 125 (1):197-218.

Bellini A. & Mastrorilli V. I. 1975. — Les corallinacées des coupes basales du Miocène de Bonifacio. *Bulletins de la Société des sciences historiques et naturelles de la Corse* 615: 33-59.

Binda P. L. 1973. — Form and internal structure of recent algal nodules (rhodolites) from Bermuda: a discussion. *Journal of Geology* 81 (2): 283. https://doi.org/10.1086/627842

Bosellini A. & Ginsburg R. N. 1971. — Form and internal structure of recent algal nodules (rhodoliths) from Bermuda. *Journal of Geology* 79 (6): 669-682. https://doi.org/10.1086/627697

Bosence D. W. J. 1976. — Ecological studies on two unattached coralline algae from western Ireland. *Paleontology* 19: 365-395. https://www.biodiversitylibrary.org/page/49770844

Bosence D. W. J. 1983a. — Description and classification of rhodoliths (rhodoids, rhodolites), *in* Peryt T. M. (ed.), *Coated Grains.* Springer-Verlag, New York: 217-224. https://doi.org/10.1007/978-3-642-68869-0_19

Bosence D. W. J. 1983b. — The ocurrence and ecology of recent rhodoliths, *in* Peryt T. M. (ed.), *Coated Grains.* Springer-Verlag, Berlin: 225-242. https://doi.org/10.1007/978-3-642-68869-0_20

Bosence D. W. J. 1991. — Coralline algae: mineralization, taxonomy and palaeoecology, *in* Riding R. (ed.), *Calcareous Algae and Stromatolites*. Springer, Berlin, Heidelberg: 98-113. https://doi.org/10.1007/978-3-642-52335-9_5

Bourrouilh Le Jan F. G. & Hottinger L. C. 1988. — Occurrence of rhodoliths in the tropical Pacific — a consequence of Mid-Miocene paleo-oceanographic change. *Sedimentary Geology* 60 (1-4): 355-367. https://doi.org/10.1016/0037-0738(88)90130-3

Bracchi V. A., Angeletti L., Marchese F., Taviani M., Cardone F., Hajdas I., Grande V., Prampolini M., Caragnano A., Corselli C. & Basso D. 2019. — A resilient deep-water rhodolith bed off the Egadi Archipelago (Mediterranean Sea) and its actuopaleontological significance. *Alpine and Mediterranean Quaternary* 32 (2): 131-150. https://doi.org/10.26382/AMQ.2019.09

Bracchi V. A., Caronni S., Meroni A. N., Burguett E. G., Atzori F., Cadoni N., Marchese F. & Basso D. 2022. — Morphostructural Characterization of the Heterogeneous Rhodolith Bed at the Marine Protected Area "Capo Carbonara" (Italy) and Hydrodynamics. *Diversity* 14 (1): 51. https://doi.org/10.3390/d14010051

Braga J. C. 2017. — Neogene rhodoliths in the Mediterranean basins, *in* Riosmena-Rodríguez R., Nelson W. & Aguirre J. (eds), *Rhodolith/Maërl Beds: A Global Perspective, Basel.* Springer, Cham: 169-193. https://doi.org/10.1007/978-3-319-29315-8_7

Braga J. C. & Martín J. M. 1988. — Neogene coralline-algal growth-forms and their palaeoenvironments in the Almanzora River Valley (Almeria S.E. Spain). *Palaeogeography, Palaeoclimatology, Palaeoecology* 67 (3-4): 285-303. https://doi.org/10.1016/0031-0182(88)90157-5

Braga J. C. & Aguirre J. 2001. — Coralline algal assemblages in Upper Neogene reef and temperate carbonates in southern Spain. *Palaeogeography, Palaeoclimatology, Palaeoecology* 175 (1-4): 27-41. https://doi.org/10.1016/S0031-0182(01)00384-4

Braga J. C. & Aguirre J. 2004. — Coralline algae indicate Pleistocene evolution from deep, open platform to outer barrier reef environments in the northern Great Barrier Reef margin. *Coral Reefs* 23: 547-558. https://doi.org/10.1007/s00338-004-0414-x

Braga J. C. & Bassi D. 2007. — Neogene history of Sporolithon Heydrich (Corallinales, Rhodophyta) in the Mediterranean region. *Palaeogeography, Palaeoclimatology, Palaeoecology* 243 (1-2): 189-203. https://doi.org/10.1016/j.palaeo.2006.07.014

Braga J. C., Bosence D. W. J. & Steneck R. S. 1993. — New anatomical characters in fossil coralline algae and their taxonomic implications. *Palaeontology* 36 (3): 535-547.

Braga J. C., Betzler C., Martín J. M. & Aguirre J. 2003. — Spit-platform temperate carbonates: the origin of landward downlapping beds along a basin margin (Lower Pliocene, Carboneras Basin, SE Spain). *Sedimentology* 50 (3): 553-563. https://doi.org/10.1046/j.1365-3091.2003.00564.x

Braga J. C., Vescogni A., Bosellini F. R. & Aguirre J. 2009. — Coralline algae (Corallinales, Rhodophyta) in western and central Mediterranean Messinian reefs. *Palaeogeography, Palaeoclimatology, Palaeoecology* 275 (1-4): 113-128. https://doi.org/10.1016/j.palaeo.2009.02.022

Braga J. C., Bassi D. & Piller W. E. 2010. — Paleoenvironmental significance of Oligocene-Miocene coralline red algae – a review, *in* Mutti M., Piller W. E. & Betzler C. (eds), Carbonate system during the Oligocene-Miocene Cli-matic Transition. *International Association of Sedimentologists* Special Publication 42: 165-182. https://doi.org/10.1002/9781118398364.ch10

Brandano M., Vannucci G., Pomar L. & Obrador A. 2005. — Rhodolith assemblages from the lower Tortonian carbonate ramp of Menorca (Spain): environmental and paleoclimatic implications. *Palaeogeography, Palaeoclimatology, Palaeoecology* 226 (3-4): 307-323. https://doi.org/10.1016/j.palaeo.2005.04.034

Brandano M., Vannucci G. & Mateu-Vicens G. 2007. — Le alghe rosse calcaree come indicatori paleoambientali: l'esempio della rampa carbonatica Laziale-Abruzzese (Burdigaliano, Appenino centrale). *Bollettino della Società Geologica Italiana* 126: 55-69.

Chamberlain Y. M. & Irvine L. M. 1994. — Lithophylloideae Setchell, *in* Irvine L. M. & Chamberlain Y. M. (eds), *Seaweeds of the British Isles, Rhodophyta Part 2B Corallinales, Hildenbrandiales.* Vol. 1. HMSO, London: 58-112.

Chelaru R. & Bucur I. I. 2016. — The taxonomy of middle Miocene red algae from the Gârbova de Sus Formation (Transylvanian Basin, Romania). *Carnets de Geologie* 16 (11): 307-336. https://doi.org/10.4267/2042/60121

Chelaru R., Săsăran E., Tămaș T., Bălc R., Bucur I. I. & Pleș G. 2019. — Middle Miocene carbonate facies with rhodoliths from the NW Transylvanian Basin (Vălenii Șomcutei Cave, Romania). *Facies* 65 (4): 1-16. https://doi.org/10.1007/s10347-018-0546-z

Civitelli G. & Brandano M. 2005. — Atlante delle litofacies e modello deposizionale dei Calcari a Briozoi e Litotamni nella Piattaforma carbonatica laziale-abruzzese. *Bollettino-Societa Geologica Italiana* 124 (3): 611-643.

Coletti G. & Basso D. 2020. — Coralline algae as depth indicators in the Miocene carbonates of the Eratosthenes Seamount (ODP Leg 160, Hole 966F). *Geobios* 60: 29-46. https://doi.org/10.1016/j.geobios.2020.03.005

Coletti G., Basso D., Frixa A. & Corselli C. 2015. — Transported rhodoliths witness the lost carbonate factory: a case history from the Miocene Pietra da Cantoni limestone (NW Italy). *Rivista Italiana di Paleontologia e Stratigrafi* 121 (3): 345-368. https://doi.org/10.13130/2039-4942/6522

Coletti G., Basso D. & Corselli C. 2018. — Coralline algae as depth indicators in the Sommières Basin (early Miocene, Southern France). *Geobios* 51: 15-30. https://doi.org/10.1016/j.geobios.2017.12.002

Conti S. 1943. — Contributo allo studio delle Corallinacee del terziario italiano. II. Le Corallinacee del Miocene del Bacino Ligure-Piemontese. *Palaeontographia Italica* 41: 37-61.

Conti S. 1946. — Le Corallinacee del calcare miocenico (Leithakalk) del bacino di Vienna. *Publication 1st Geology University of Genova, Series A (Paleontology)* 2: 31-68.

Croizé D., Renard F., Bjørlykke K. & Dysthe D. K. 2010. — Experimental calcite dissolution under stress: evolution of grain contact microstructure during pressure solution creep. *Journal of Geophysical Research* 115 (B9): B09207. https://doi.org/10.1029/2010JB000869

Denizot M. 1968. — *Les algues floridées encroûtantes (à l'exclusion des Corallinacées).* Thèse, Laboratoire de Cryptogamie, Muséum national d'Histoire naturelle, Paris, 310 p.

Esteban M. 1996. — An overview of Miocene reefs from Mediterranean areas: General trends and facies models, *in* Franseen E. K. Esteban M., Ward W. C. & Rouchy J.-M. (eds), Models for carbonate stratigraphy from Miocene reef complexes of Mediterranean regions: SEPM (Society for Sedimentary Geology). *Concepts in Sedimentology and Paleontology* 5: 3-53. https://doi.org/10.2110/csp.96.01.0003

Foslie M. 1898. — List of species of the Lithothamnia. *Det Kongelige Norske Videnskabers Selskab Skrifter* 3: 1-11.

Foslie M. 1903. — Den botaniske samling. *Det Kongelige Norske Videnskabers Selskabs Skrifter* 1902: 23-25.

Foslie M. 1908. — Algologiske notiser. V. *Kongelige Norske Videnskabers Selskabs Skrifter* 7: 1-20.

Foslie M. 1909. — Algologiske notiser. VI. Det Kongelige Norske Videnskabers Selskabs Skrifter 1909. *Trondheim* 2: 1-63.

Foster M. S. 2001. — Rhodoliths: between rocks and soft places. *Journal of Phycology* 37 (5): 659-667. https://doi.org/10.1046/j.1529-8817.2001.00195.x

Foster M. S., Riosmena-Rodriguez R., Steller D. S. & Woelkerling W. J. 1997. — Living Rhodolith Beds in the Gulf of California and Their Implications for Paleoenvironmental Inter-

pretation, *in* Johnson M. E. & Ledesma-Vásquez J. (eds), Pliocene Carbonates and Related Facies Flanking the Gulf of California, Baja California. *Geological Society of America Special Paper* 318: 127-139. https://doi.org/10.1130/0-8137-2318-3.127

Francavilla F., Frascari Ritondale Spano F. & Zecchi R. 1970. — Alghe e Macroforaminiferi al limite Eocene-Oligocene presso Barbarano (Vicenza). *Giornale di Geologia* 36: 653-686.

Fravega P., Giammarino S., Piazza M., Russo A. & Vannucci G. 1987. — Significato paleoecologico degli episodi coralgali a Nord di Sassello. Nuovi dati per una ricostruzione paleogeografico-evolutiva del margine meridionale del Bacino Terziario del Piemonte. *Atti della Società Toscana di Scienze Naturali -* Memorie Serie *A* 94: 19-76.

Fravega P., Giammarino S., Traverso G. & Vannucci G. 1988. — Insediamenti coralgali e loro significato nell'evoluzione delle conoidi oligoceniche della Val Lemme (Bacino Terziario del Piemonte), *in* Robba E. (ed.), *Atti IV Simposio "Ecologia e Paleoecologia delle Comunità Bentoniche".* Bollettino del Museo Regionale di Scienze Naturali di Torino, Sorrento: 199-221.

Fravega P., Piazza M. & Vannucci G. 1989. — *Archaeolithothamnium* Rothpletz indicatore ecologico-stratigrafico? *in* Di Geronimo I. (ed.), *Atti del 3° Simposio di Ecologia e Paleoecologia delle Comunità Bentoniche.* Catania: 729-743.

Gale L. 2009. — Non-geniculate coralline algae (Corallinales, Rhodophyta) from the Lower Oligocene of Poljšica pri Podnartu (northern Slovenia). *Rivista Italiana Di Paleontologia e Stratigrafia* 115 (1): 87-100.

Ghosh A. K., Chakraborty A. & Mazumder A. 2017. — *Halimeda* bioherms from the Serravallian (Middle Miocene) of Little Andaman Island, India. *Micropaleontology* 63 (1): 67-76. https://www.jstor.org/stable/26645544

Ginsburg R. N. & Bosellini A. 1973. — Form and internal structure of recent algal nodules (rhodolites) from Bermuda: a reply. *Journal of Geology* 81 (2): 239. https://doi.org/10.1086/627843

Gray J. E. 1864. — Handbook of British water-weeds or algae. R. Hardwicke, London, 123 p.

Guiry M. D. & Guiry G. M. 2018. — AlgaeBase. World-wide electronic publication, National University of Ireland, Galway. Available at: https://www.algaebase.org (accessed on 19 May 2022)

Halfar J. & Mutti M. 2005. — Global dominance of coralline red-algal facies: a response to Miocene oceanographic events. *Geology* 33 (6): 481-484. https://doi.org/10.1130/G21462.1

Harvey A. S., Woelkerling W. J. & Millar A. J. K. 2009. — The genus *Lithophyllum* (Lithophylloideae, Corallinaceae, Rhodophyta) in south-eastern Australia, with the description of *L. riosmenae*, sp. nov. *Australian Systematic Botany* 22: 296-317.

Heydrich F. 1897. — *Corallinaceae, insbesonde-re Melobesieae.* Berichte der deutsche botanischen Gesellschaft, Wien, Band XV: 34-70.

Hrabovský J., Basso D. & Doláková N. 2015. — Diagnostic characters in fossil coralline algae (Corallinophycidae: Rhodophyta) from the Miocene of southern Moravia (Carpathian Foredeep, Czech Republic). *Journal of Systematic Paleontology* 14 (6): 1-27. https://doi.org/10.1080/14772019.2015.1071501

Iryu Y. 1992. — Fossil non-articulated coralline algae as depth indicators for the Ryukyu Group. *Transactions and Proceedings of the Palaeontological Society of Japan* 167: 1165-1179.

Iryu Y., Takahashi,Y., Fujita K., Camoin G., Caboich G., Matsuda H., Sato T., Sugihara K., Webster J. M. & Westphal H. 2010. — Sealevel history recorded in the Pleistocene carbonate sequence in IODP Hole 310-M0005D, off Tahiti. *Island Arc* 19 (4): 690-706. https://doi.org/10.1111/j.1440-1738.2010.00737.x

Jesionek M. B., Bahia R. G., Hernández-Kantún J. J., Adey W. H., Yoneshigue-Valentin Y., Longo L. L. & Amado-Filho G. M. 2016. — A taxonomic account of non-geniculate coralline algae (Corallinophycidae, Rhodophyta) from shallow reefs of the Abrolhos Bank, Brazil. *Algae* 31 (4): 317-340. https://doi.org/10.4490/algae.2016.31.11.16

JOHANSEN H. W. 1974. — Articulated coralline algae. *Oceanography and Marine Biology – An Annual Review* 12: 77-127.

JOHNSON J. H. 1957. — Geology of Saipan, Mariana Islands, Pt. 3, Paleontology: Calcareous algae. U.*S. Geological Survey Professional Paper* 280: 209-246.

KATO A. & BABA M. 2019. — Distribution of *Lithophyllum kuroshioense* sp. nov., *Lithophyllum subtile* and *L. kaiseri* (Corallinales, Rhodophyta), but not *L. kotschyanum*, in the northwestern Pacific Ocean. *Phycologia* 58 (2): 1-13. https://doi.org/10.1080/00318884.2019.1643200

KATO A. M. BABA & S. SUDA. 2011. — Revision of the Mastophoroideae (Corallinales, Rhodophyta) and polyphyly in nongeniculate species widely distributed on Pacific coral reefs. *Journal of Phycology* 47 (3): 662-672. https://doi.org/10.1111/j.1529-8817.2011.00996.x

KONAR B. & FOSTER M. S. 1992. — Distribution and recruitment of subtidal geniculate coralline algae. *Journal of Phycology* 28 (3): 273-280. https://doi.org/10.1111/j.0022-3646.1992.00273.x

KUNDAL P. & HUMANE S. K. 2003. — *Corallina*, a geniculate coralline alga from Middle Eocene to Lower Miocene of Kachchh, Gujarat, India, *in* KUNDAL P. (ed.), *Recent Developments in Indian Micropaleontology. Gondwana Geological Magazine* Special volume 6: 261-275.

KUNDAL P., HUMANE S. S. & HUMANE S. K. 2011. — Calcareous algae from the Miliolite Formation (Middle Pleistocene) of Diu, Saurashtra. *Journal of the Palaeontological Society of India* 56 (2): 181.

KUNDAL P., MILIND P. K. & HUMANE S. K. 2016. — Nongeniculate Coralline Algae from Early Middle Miocene Offshore Sequence of Kachchh Basin, Western India: Paleoenvironmental Significance. *Journal of the Geological Society of India* 88: 39-46. https://doi.org/10.1007/s12594-016-0456-z

KÜTZING F. T. 1841. — Ueber die "Polypieres calcifères" des Lamouroux, *in* FISHER K. C. F. (ed.), *Zu der öffentlichen Prüfung sämmtlicher Classen der Realschule zu Nordhausen.* Nordhausen, Realschule: 3-34.

KÜTZING F. T. 1843. — *Phycologia Generalis : Oder Anatomie, Physiologie und Systemkunde der Tange.* F. A. Brockhaus, Leipzig, 458 p. https://doi.org/10.5962/bhl.title.4746

LAMOUROUX J. V. F. 1812. — Extrait d'un memoire sur la classification des Polypiers coralligènes non entierement pierreux. *Nouveau Bulletin des Sciences, publié par la Société Philomatique de Paris* 3 (63): 181-188.

LAMOUROUX J. V. F. 1816. — *Histoire des polypiers coralligènes flexibles, vulgairement nommés zoophytes.* Imprimerie de F. Poisson, Caen, 560 p. https://doi.org/10.5962/bhl.title.11172

LE GALL L. & SAUNDERS G. W. 2007. — A nuclear phylogeny of Florideophyceae (Rhodophyta) inferred from combined EF2, small subunit and large subunit ribosomal DNA: establishing the new red algal subclass Corallinophycidae. *Molecular Phylogenetics and Evolution* 43 (3): 1118-1130. https://doi.org/10.1016/j.ympev.2006.11.012

LE GALL L., PAYRI C. E., BITTNER C. E. & SAUNDERS G. W. 2009. — Multigene polygenetic analyses support recognition of the Sporolithales, ord. nov. *Molecular Phylogenetics and Evolution* 54 (1): 302-305. https://doi.org/10.1016/j.ympev.2009.05.026

LEE R. E. 1989. — *Phycology.* 2nd Edition. Cambridge University Press, Cambridge, 645 p.

LEMOINE M. P. 1924. — Contribution a l'étude des Corallinacées fossiles. VII. Mélobesiées miocenes recueillies par M. Bourcart en Albanie. *Bulletin de la Société Géologique de France* 23: 275-283.

LEMOINE M. 1928. — Un nouveau genre de Mélobésiées. *Mesophyllum. Bulletin Societé Botanique de France* 75 (2): 251-254. https://doi.org/10.1080/00378941.1928.10836268

LESZCZYŃSKI S., KOŁODZIEJ B., BASSI D., MALATA E. & GASIŃSKI M. A. 2012. — Origin and resedimentation of rhodoliths in the Late Paleocene flysch of the Polish Outer Carpathians. *Facies* 58 (3): 367-387. https://doi.org/10.1007/s10347-012-0302-8

LI Y., YU K., BIAN L., FAN T., WANG R., JIANG W., XU S., ZHANG Y. & YANG Y. 2021. — Paleo-water depth variations since the Pliocene as recorded by coralline algae in the South China Sea. *Palaeogeography, Palaeoclimatology, Palaeoecology* 562: 110107. https://doi.org/10.1016/j.palaeo.2020.110107

LINNAEUS C. 1758. — *Systema naturae.* 12th Edition. Laurentii Salvi, Stockholm, 824 p.

LITTLER M. M., LITTLER D. S. & HANISAK M. D. 1990. — Deepwater rhodolith distribution, productivity, and growth history at sites of formation and subsequent degradation. *Journal of Experimental Marine Biology and Ecology* 150 (2): 163-182. https://doi.org/10.1016/0022-0981(91)90066-6

LÜBBERS J., KUHNT W., HOLBOURN A. E., BOLTON C. T., GRAY E., USUI Y. & ANDERSEN N. 2019. — The middle to late Miocene "Carbonate Crash" in the equatorial Indian Ocean. *Paleoceanography and Paleoclimatology* 34 (5): 813-832.

LUND M., DAVIES P. J. & BRAGA J. C. 2000. — Coralline algal nodules off Fraser Island, Eastern Australia. *Facies* 42: 25-34. https://doi.org/10.1007/BF02562564

MANKER J. P. & CARTER B. D. 1987. — Paleoecology and paleogeography of an extensive rhodolith facies from the lower Oligocene of South Georgia and north Florida. *Palaios* 592: 181-188. https://doi.org/10.2307/3514647

MARRACK E. C. 1999. — The relationship between water motion and living rhodolith beds in the southwestern Gulf of California, Mexico. *Palaios* 14: 159-171. https://doi.org/10.2307/3515371

MARTÍN J. M., BRAGA ALARCÓN J. C., KONISHI K. & PIGRAM C. J. 1993. — A model for the development of rhodoliths on platforms influenced by storms: middle Miocene carbonates of the Marion Plateau (northeastern Australia). *Proceedings of the Ocean Drilling Program, Scientific Results* 133: 455-460. http://hdl.handle.net/10481/22939

MASTRORILLI V. I. 1967. — *Lithophyllum contii*: nuova specie di Corallinacea diffusa nella formazione oligocenica di Bric Mazzapiede, presso Prasco (Acqui). *Atti dell'Istituto di Geologia della Università di Genova* 4: 475-488.

MASTRORILLI V. I. 1968. — Nuovo contributo allo studio delle Corallinacee dell'Oligocene Ligure-Piemontese: i reperti della tavoletta Ponzone. *Atti Ist. Geology University of Genova* 5 (2): 153-106.

MATEO-CID L. E., MENDOZA-GONZÁLEZ A. C. & GABRIELSON P. W. 2014. — *Neogoniolithon* (Corallinales, Rhodophyta) on the Atlantic coast of Mexico, including *N. siankanensis* sp. nov. *Phytotaxa* 190 (1): 64-93. https://doi.org/10.11646/phytotaxa.190.1.7

MINNERY G. A., REZAK R. & BRIGHT T. J. 1985. — Depth zonation and growth forms of crustose coralline algae: Flower Garden Banks, Northwestern Gulf of Mexico, *in* TOOMEY D. F. & NITECKI M. H. (eds), *Paleoalgology: Contemporary Research and Applications,* Springer, New York: 237-246. https://doi.org/10.1007/978-3-642-70355-3_18

MISRA U., KISHORE S., SINGH S. K., MISRA P. K. & JAUHRI A. K. 2016. — New Record of Coralline Algae from the Holocene sediments of Agatti Island, Lakshadweep, India. *Journal of the Geological Society of India* 87: 308-316. https://doi.org/10.1007/s12594-016-0397-6

MOUSSAVIAN E. 1984. — Upper Cretaceous and Paleogene Pebbles of the Angerberg Beds (Late Oligocene, Unterinntal, Northern Alps). *Facies* 10: 1-86. https://doi.org/10.1007/BF02536688

NÄGELI C. 1858. — Die Stärkekörner, *in* NÄGELI C. & KRAMER C. (eds), *Pflanzenphysiologische Untersuchungen.* Friedrich Schulthess, Zürich, 624 p.

NEBELSICK J. H. & BASSI D. 2000. — Diversity, growth forms and taphonomy: key factors controlling the fabric of coralline algae dominated shelf carbonates. *Geological Society, London* 178 (1): 89-107. https://doi.org/10.1144/GSL.SP.2000.178.01.07

NEBELSICK J. H., STINGL V. & RASSER M. 2001. — Autochthonous facies and allochthonous debris flows compared: Early Oligocene carbonate facies patterns of the Lower Inn Valley (Tyrol, Austria). *Facies* 44 (1): 31. https://doi.org/10.1007/BF02668165

Nebelsick J. H., Rasser M. W. & Bassi D. 2005. — Facies dynamics in Eocene to Oligocene circumalpine carbonates. *Facies* 51: 197-217. https://doi.org/10.1007/s10347-005-0069-2

Neill K. F., Nelson W. A., D'archino R., Leduc D. & Farr T. J. 2015. —Northern New Zealand rhodoliths: assessing faunal and floral diversity in physically contrasting beds. *Marine Biodiversity* 45: 63-75. https://doi.org/10.1007/s12526-014-0229-0

Nelson W. A. 2009. — Calcified macroalgae critical to coastal ecosystems and vulnerable to change: a review. *Marine & Freshwater Research* 60 (8): 787-801. http://doi.org/10.1071/MF08335

Novak V. & Renema W. 2018. — Ecological tolerances of Miocene larger benthic foraminifera from Indonesia. *Journal of Asian Earth Sciences* 151: 301-323. https://doi.org/10.1016/j.jseaes.2017.11.007

Piller W. E. 2003.— Miocene carbonates in the western central Paratethys, an unexpected development, *in* Bassi D. (ed.), Oligo-Miocene shallow water carbonates: biogenic components and facies. *Annali dellUniversità di Ferrara, sezione Scienze della Terra* 10: 19-20.

Pomar L., Baceta J., Hallock P., Mateu-Vicens G. & Basso D. 2017. — Reef building and carbonate production modes in the west-central Tethys during the Cenozoic. *Marine and Petroleum Geology* 83: 261-304. https://doi.org/10.1016/j.marpetgeo.2017.03.015

Quaranta F., Vannucci G. & Basso D. 2007. — *Neogoniolithon contii* comb. nov. based on the taxonomic re-assessment of Mastrorilli's original collections from the Oligocene of NW Italy (Tertiary Piedmont Basin). *Rivista Italiana di paleontologia e stratigrafia* 113 (1): 43-55. https://doi.org/10.13130/2039-4942/6357

Rasser M. 1994. — Facies and palaeoecology of rhodoliths and acervulinid macroids in the Eocene of the Krappfeld (Austria). *Beiträge Zur Paläontologie* 19: 191-217.

Rasser M. W. & Piller W. E. 1997. — Depth distribution of calcareous encrusting associations in the northern Red Sea (Safaga, Egypt) and their geological implications. *Proceedings of the 8th International Coral Reef Symposium, Panama* 1: 743-748.

Rasser M. W. & Piller W. E. 1999. —Application of neontological taxonomic concepts to late Eocene coralline algae (Rhodophyta) of the Austrian Molasse Zone. *Journal of Micropalaeontology* 18 (1): 67-80. https://doi.org/10.1144/jm.18.1.67

Rasser M. W. & Nebelsick J. H. 2003. — Provenance analysis of Oligocene autochthonous and allochthonous coralline algae: a quantitative approach towards reconstructing transported assemblages. *Palaeogeography, Palaeoclimatology, Palaeoecology* 201 (1-2): 89-111. https://doi.org/10.1016/S0031-0182(03)00512-1

Rasser M. W. & Piller W. E. 2004. — Crustose algal frameworks from the Eocene Alpine Foreland. *Palaeogeography Palaeoclimatology Palaeoecology* 206 (1-2): 21-39. https://doi.org/10.1016/j.palaeo.2003.12.018

Rebelo A. C., Rasser M., Riosmena-Rodríguez R., Neto A. I. & Avila S. 2014. — Rhodolith forming coralline algae in the Upper Miocene of Santa Maria Island (Azores, NE Atlantic): a critical evaluation. *Phytotaxa* 190 (1): 370-382. https://doi.org/10.11646/phytotaxa.190.1.22

Rebelo A. C., Johnson M. E., Rasser M. W., Silva L., Melo C. S. & Ávila S. P. 2021. — Global biodiversity and biogeography of rhodolith-forming species. *Frontiers of Biogeography* 13 (1): e50646. https://doi.org/10.21425/F5FBG50646

Riosmena-Rodríguez R. 2017. — Natural History of Rhodolith/Maërl Beds: Their role in near-shore biodiversity and management, *in* Riosmena-Rodriguez R., Nelson W. & Aguirre J. (eds), *Rhodolith/Maërl Beds: a global perspective*. Springer, Cham: 3-26. https://doi.org/10.1007/978-3-319-29315-8_1

Riosmena-Rodríguez R., Nelson W. & Aguirre J. 2017. — *Rhodolith/Maërl beds: a global perspective*. Springer (coll. Coastal Research Library; 15), Cham, 368 p. https://doi.org/10.1007/978-3-319-29315-8

Roozpeykar A. & Moghaddam I. M. 2016. — Benthic foraminifera as biostratigraphical and paleoecological indicators: An example from Oligo-Miocene deposits in the SW of Zagros basin, Iran. *Geoscience Frontiers* 7 (1): 125-140. https://doi.org/10.1016/j.gsf.2015.03.005

Sañé E., Chiocci F. L., Basso D. & Martorelli E. 2016. — Environmental factors controlling the distribution of rhodoliths: an integrated study based on seafloor sampling, ROV and side scan sonar data, offshore the W-Pontine Archipelago. *Continental Shelf Research* 129: 10-22. https://doi.org/10.1016/j.csr.2016.09.003

Sarkar S. & Ghosh A. K. 2015. — Evaluation of coralline algal diversity from the Serravallian carbonate sediments of Little Andaman Island (Hut Bay), India. *Carbonate and Evaporites* 30: 13-24. https://doi.org/10.1007/s13146-014-0190-9

Sarkar S., Ghosh A. K. & Narasimha Rao G. M. 2016. — Coralline Algae and Benthic Foraminifera from the Long Formation (middle Miocene) of the Little Andaman Island, India: Biofacies Analysis, Systematics and Palaeoenvironmental Implications. *Journal of the Geological Society of India* 87: 69-84. https://doi.org/10.1007/s12594-016-0375-z

Sarma A., Ghosh A. K & Sarkar S. 2014. — First record of Coralline Red Algae from the Kopili Formation (late Eocene) of Meghalaya, N-E India. *National Academy Science Letters* 37: 503-507. https://doi.org/10.1007/s40009-014-0267-y

Schneider C. W. & Wynne M. J. 2019. — Fourth addendum to the synoptic review of red algal genera. *Botanica Marina* 62 (4): 355-367. https://doi.org/10.1515/bot-2019-0003

Setchell W. A. 1943. — Mastophora and the Mastophoreae: genus and subfamily of Corallinaceae. *Proceedings of the National Academy of Sciences of the United States of America* 29 (5): 127-135. https://doi.org/10.1073/pnas.29.5.127

Setchell W. A. & Mason L. R. 1943. — *Gonioli-thon* and *Neogoniolithon*: two genera of crustaceous coralline algae. *Proceedings of the National Academy of Sciences* 29 (3-4): 87-92.

Sharma V. & Srinivasan M. S. 2007. — *Geology of Andaman-Nicobar: The Neogene.* Capital Publishing Company, New Delhi, 164 p.

Silva H. W. & Johansen H. W. 1986. — A reappraisal of the order Corallinales (Rhodophyceae). *British Phycological Journal* 21 (3): 245-254.

Srinivasan M. S. 1988. — Late Cenozoic sequences of Andaman-Nicobar Islands: Their regional significance and correlation. *Indian Journal of Geology* 60 (1): 11-34.

Srinivasan M. S. & Chatterjee B. K. 1981. — Stratigraphy and depositional environments of Neogene limestones of Andaman-Nicobar Islands, Northern Indian Ocean. *Journal of the Geological Society of India* 22 (11): 536-546.

Steller D. L. & Foster M. S. 1995. — Environmental factors influencing distribution and morphology of rhodoliths in Bahia Concepcion B.C.S., México. *Journal of Experimental Marine Biology and Ecology* 194 (2): 201-212. https://doi.org/10.1016/0022-0981(95)00086-0

Townsend R. A. & Huisman J. M. 2018. — Coralline algae, *in* Huisman J. M. (ed.), *Algae of Australia. Marine Benthic Algae of North-Western Australia*. Vol. 2. Red algae. ABRS & CSIRO Publishing, Canberra; Melbourne: 83-146 p.

Turner J. A. & Woelkerling W. J. 1982. — Studies on the *Mastophora-Lithoporella* complex (Corallinaceae, Rhodophyta) I. meristems and thallus structure and development. *Phycologia* 21 (3): 201-217. https://doi.org/10.2216/i0031-8884-21-3-201.1

Van Den Hoek C., Mann D. G. & Jahns H. M. 1995. — *Algae. An introduction to phycology.* Cambridge University Press, Cambridge, 623 p.

Van Der Merwe E. & Maneveldt G. W. 2014. — The genus *Phymatolithon* (Hapalidiaceae, Corallinales, Rhodophyta) in South Africa, including species previously ascribed to *Leptophytum*. *South African Journal of Botany* 90: 170-192. https://doi.org/10.1016/j.sajb.2013.11.004

Van Der Merwe E. & Maneveldt G. W. 2015. — A modern account of the South African non-geniculate Lithophylloideae (Corallinales, Corallinophycidae, Rhodophyta). *South African Journal of Botany* 103: 247-267.

Vannucci G., Piazza M., Fravega P. & Chiesa I. 1994. — Calcareous Rhodophyceae from the "facies astiane" (Pliocene) of Valle San Bartolomeo (Alessandria, N.W. Italy), *in* Matteucci R., Carboni M. G. & Pignatti J. S. (eds), Studies on Ecology and Paleoecology of Benthic Communities. *Bulletin of the Society of Paleontology* 2: 351-364.

Vannucci G., Piazza M., Fravega P. & Basso D. 2000. — Revision and re-documentation of M. AIROLDI's species of *Archaeolithothamnium* from the Tertiary Piedmont basin (NW Italy). *Rivista Italiana di Paleontologia e Stratigrafia*, 106 (2): 191-202.

Vannucci G., Quaranta F. & Basso D. 2010. — Revision and re-documentation of M. Airoldi's species of *Lithothamnion* from the Tertiary Piedmont Basin (NW Italy). *Rivista Italiana di Paleontologia e Stratigrafia* 116: 223-225.

Verheij E. 1993. — The genus *Sporolithon* (Sporolithaceae fam. nov., Corallinales, Rhodo-phyta) from the Spermonde Archipelago, Indonesia. *Phycologia* 32 (3): 184-196. https://doi.org/10.2216/i0031-8884-32-3-184.1

Vieira-Pinto T., Oliveira M. C., Bouzon J., Sissini M., Richards J. L., Riosmena-Rodrí´ Guez & Horta P. A. 2014. — *Lithophyllum* species from Brazilian coast: range extension of *Lithophyllum margaritae* and description of *Lithophyllum atlanticum* sp. nov. (Corallinales, Corallinophycidae, Rhodophyta). *Phytotaxa* 190 (1): 355-369. https://doi.org/10.11646/phytotaxa.190.1.21

Woelkerling W. J. 1988. — *The Coralline Red Algae: An analysis of the genera and subfamilies of nongeniculate Corallinaceae*. British Museum (Natural History), London; Oxford University Press, London, 268 p.